

$D_s \rightarrow f_0$ form factors and the $D_s^+ \rightarrow [\pi\pi]_S e^+ \nu_e$ decay from light-cone sum rules

Shan Cheng^{1,2,3,*} and Shu-Lei Zhang^{1,2,3,†}

¹*School of Physics and Electronics, Hunan University, 410082 Changsha, China.*

²*School for Theoretical Physics, Hunan University, 410082, Changsha, China.*

³*Hunan Provincial Key Laboratory of High-Energy Scale Physics and Applications, 410082 Changsha, China.*

(Dated: July 6, 2023)

In this paper we revisit $D_s \rightarrow f_0$ form factors from the light-cone sum rules with the light meson light-cone distribution amplitudes. The main motivation of this study is the differential decay width of $D_s \rightarrow [\pi\pi]_S e \nu_e$ measured recently by BESIII collaboration and the $D_s \rightarrow f_0$ form factor extracted under the intermediate resonant model. Our result of the differential width of $D_s^+ \rightarrow f_0(\rightarrow [\pi\pi]_S) e^+ \nu_e$ decay obtained under the narrow width approximation is a litter bit lower than the data, the result obtained under the resonant Flatté model is in consistent with the data while shows a litter bit larger, indicating a sizable mixing $\sim 20^\circ$ between $\bar{s}s$ and $\bar{u}u + \bar{d}d$ of f_0 . In order to obtain a model independent prediction, we suggest to calculate $D_s \rightarrow [\pi\pi]_S$ form factors with the isoscalar scalar dipion light-cone distribution amplitudes. Our calculation of $D_s \rightarrow [\pi\pi]_S$ form factors is carried out at the leading twist level due to the finite knowledge of dipion system, the result of differential width shows a moderate evolution in contrast to that obtained from the narrow width approximation and the Flatté model, revealing a bright prospect to study the four-body leptonic decays of heavy mesons with the dimeson light-cone distribution amplitudes.

I. INTRODUCTION

Weak decays of hadrons containing at least a valence bottom or charm quarks play an important role in the precise examination of standard model (SM) and offer one of the best chance for the discovery of new physics (NP) beyond standard model, in which the semileptonic D_s weak decays provide the clear enviroment to study the structure of light hadrons [1]. For examples, the semileptonic decay with $D_s \rightarrow \eta^{(\prime)}$ transition provides an opportunity to study the η - η' mixing [2, 3], the decay deduced by $D_s \rightarrow f_0$ and $D_s \rightarrow a_0$ transitions could help us to understand the composition figure of scalar mesons [4–6] and the isospin-violated f_0 - a_0 mixing [7, 8]. In this work, we focus on the $D_s^+ \rightarrow f_0 e^+ \nu_e$ decay by considering the width effect in the differential width measurements.

From the spectral analysis, the underlying assignments of scalar mesons like $f_0(980)$ is still not clear. Pictures like the tetraquark [9, 10], the gluonball [11], the hybrid state [12] and the molecule state [13] are all discussed, in which the tetraquark assignment is more favorite nowadays. The case is different in the B meson decay where f_0 is energetic and the process happens with large recoiling, in this case the conventional $q\bar{q}$ assignment is the favorite one because the possibility to form a tetra-quark state is power suppressed with comparing to the state of quark pair. In the $D_s \rightarrow f_0$ decay, one may doubt the $q\bar{q}$ configuration because f_0 is not fast moving enough so that it has time to pick other $q\bar{q}$ to form a tetraquark. This is also our consideration in this paper, we take the $q\bar{q}$ configuration in the form factors calculation to check the reliability of energetic picture in charm meson decays. From the experiment side, one decade ago, CLEO collaboration published the first absolute branching fraction measurement of D_s semileptonic decay including a scalar meson in the final state. The result published firstly is $\mathcal{B}(D_s^+ \rightarrow f_0 e^+ \nu_e) \times \mathcal{B}(f_0 \rightarrow \pi^+ \pi^-) = (1.3 \pm 0.4 \pm 0.1) \times 10^{-3}$ [14] and subsequently updated to $(2.0 \pm 0.3 \pm 0.1) \times 10^{-3}$ in Ref. [15] and also in Ref. [16]. Recently, the BESIII collaboration has verified the CLEO measurement with much better accuracy, the result of product branching fraction is $\mathcal{B}(D_s^+ \rightarrow f_0 e^+ \nu_e) \times \mathcal{B}(f_0 \rightarrow \pi^0 \pi^0) = (0.79 \pm 0.14 \pm 0.03) \times 10^{-3}$ for the neutral channel [17] and $\mathcal{B}(D_s^+ \rightarrow f_0 e^+ \nu_e) \times \mathcal{B}(f_0 \rightarrow \pi^+ \pi^-) = (1.72 \pm 0.13 \pm 0.10) \times 10^{-3}$ for the charged channel [18]. More important is that BESIII extracted the $D_s \rightarrow f_0$ form factor under the Flatté resonant model with the data corresponding to an integrated luminosity of 7.33 fb^{-1} , the result at the full recoiled point is $f_+(q^2 = 0) = 0.518 \pm 0.018 \pm 0.036$ [18] with the statistical and systematic errors.

In this paper, we revisit the $D_s \rightarrow f_0(980)$ form factor under the scenario of $\bar{s}s$ and possible mixing with $\bar{u}u + \bar{d}d$. With considering the mixing angle $\theta = 20^\circ \pm 10^\circ$, the updated LCSRs calculation of $D_s \rightarrow f_0$ form factor is in consistent with the one extracted from the differential width of $D_s^+ \rightarrow f_0([\pi\pi]_S) e^+ \nu_e$ decay under the Flatté model by BESIII. while showing a litter bit larger. Our calculation is carried out at leading order of strong coupling constant. In order to estimate the next-to-leading-order (NLO) correction, we vary the charm quark mass by $\bar{m}_c(m_c) = 1.3 \pm 0.3 \text{ GeV}$ which deduces 20% – 30% additional uncertainty. We adopt the Flatté formula to discuss the width effect in semileptonic decay $D_s^+ \rightarrow f_0(\rightarrow \pi^+ \pi^-) e^+ \nu_e$ and compare the differential width to the recent measurements at BESIII [18]. In order to obtain a model independent prediction,

* Corresponding author: scheng@hnu.edu.cn

† Corresponding author: zhangshulei@hnu.edu.cn

we suggest to calculate $D_s \rightarrow [\pi\pi]_S$ form factors with dipion distribution amplitudes (2π DAs) and compare directly to the measurement without involving resonant. The q^2 dependence of $D_s^+ \rightarrow [\pi^+\pi^-]_S e^+\nu_e$ decay width indeed shows a different behavior comparing to the result obtained by resonant model. Our calculation is carried out at leading twist level due to the finite knowledge of 2π DAs, more precise measurement is highly anticipated to help us determine the subleading twist 2π DAs.

The rest of this paper is organized as follows. In the next section, the decay constant and LCDAs of scalar isoscalar meson is revisited in the framework of two-point sum rules, based on which the $D_s \rightarrow f_0$ and $B_s \rightarrow f_0$ transition form factors are calculated from the light-cone sum rules in section III. In Section IV, the chiral even generalized $\pi\pi$ distribution amplitudes is introduced and the $D_s \rightarrow [\pi\pi]_S$ form factors are obtained at leading twist level. The phenomena related to the recent BESIII measurement is presented in section III B, where the differential width is discussed under the narrow width approximation, Flatté resonant model and the direct $D_s \rightarrow [\pi\pi]$ transition. The summary is given in section V.

II. LIGHT-CONE DISTRIBUTION AMPLITUDES OF f_0

LCDAs is defined by a nonlocal matrix element sandwiched between vacuum and the onshell hadron state. Up to twist three level, the light-cone expansion of scalar meson is

$$\begin{aligned} \langle S(p_1) | \bar{q}_2 \beta(z) q_{1\alpha}(-z) | 0 \rangle &= \frac{1}{4} \int_0^1 du e^{i(2u-1)p_1 \cdot z} \left\{ p_1 \phi(u) + m_S \left[\phi^s(u) - \frac{\sigma_{\rho\delta} p_1^\rho z^\delta}{6} \phi^\sigma(u) \right] \right\}_{\beta\alpha}, \\ \langle S(p_1) | \bar{q}_2 \beta(z) g_s G_{\mu\nu}(vz) \sigma_{\rho\delta} q_{1\alpha}(-z) | 0 \rangle &= [p_{1\mu} (p_{1\rho} g_{\nu\delta}^\perp - p_{1\delta} g_{\nu\rho}^\perp)] \int \mathcal{D}\alpha_i \phi_{3S}(\alpha_i) e^{ipz(-\alpha_1 + \alpha_2 + v\alpha_3)} \\ &\quad - [p_{1\nu} (p_{1\rho} g_{\mu\delta}^\perp - p_{1\delta} g_{\mu\rho}^\perp)] \int \mathcal{D}\alpha_i \phi_{3S}(\alpha_i) e^{ipz(-\alpha_1 + \alpha_2 + v\alpha_3)}. \end{aligned} \quad (1)$$

In the definitions ϕ and $\phi^{s,\sigma}$ are the twist two and twist three LCDAs of the $\bar{q}q$ composition, respectively, ϕ_{3S} is the twist three LCDA in the $\bar{q}qg$ composition. Here $v = (u - \alpha_1)/\alpha_3$ and $\alpha_3 = 1 - \alpha_1 - \alpha_2$, the measure of three particle integral reads as

$$\int_0^u \mathcal{D}\alpha_i = \int_0^u d\alpha_1 \int_0^{1-u} \frac{d\alpha_2}{1 - \alpha_1 - \alpha_2}. \quad (2)$$

The leading twist and two particle twist three LCDAs are normalized to the vector and scale-dependent scalar decay constants, which are defined by the local matrix elements deduced by the vector and scalar currents, respectively,

$$\int_0^1 du \phi(u) = f_S, \quad \langle S(p_1) | \bar{q}_2 \gamma_\mu q_1 | 0 \rangle = f_S p_{1\mu}, \quad (3)$$

$$\int_0^1 du \phi^{(s/\sigma)}(u) = \bar{f}_S, \quad \langle S(p_1) | \bar{q}_2 q_1 | 0 \rangle = \bar{f}_S m_S. \quad (4)$$

For the neutral scalar meson like f_0, a_0 which could not be produced via the vector current, $f_S = 0$ due to the charge conjugate invariance or the conservation of vector current. This is also implied in the relation

$$\bar{f}_S = \mu_S f_s, \quad \mu_S \equiv \frac{m_S}{m_{q_2}(\mu) - m_{q_1}(\mu)}, \quad (5)$$

from which we can see that f_S vanishes in the SU(3) or isospin limit.

A. The scalar decay constant

To calculate the scalar coupling, we consider the following correlation function

$$\Pi(q) = i \int d^4x e^{iq \cdot x} \langle 0 | T \{ \bar{q}_2(x) q_1(x), \bar{q}_1(0) q_2(0) \} | 0 \rangle. \quad (6)$$

The QCD sum rule (QCDSR) of the neutral scalar coupling is quoted as [19]

$$\begin{aligned} m_S^2 \bar{f}_S^2(\mu) e^{-m_S^2/M^2} &= I_0^{\text{pert}}(s_0, M^2) + \langle \bar{q}q \rangle I_0^{(\bar{q}q)}(M^2) + \langle \alpha_s G^2 \rangle I_0^{(\alpha_s G^2)}(M^2, \mu) \\ &\quad + \langle g_s \bar{q} \sigma T G q \rangle I_0^{(g_s \bar{q} \sigma T G q)}(M^2) + \langle g_s \bar{q}q \rangle^2 I_0^{(g_s \bar{q}q)^2}(M^2) + \langle g_s^2 \bar{q}q \rangle^2 I_0^{(g_s^2 \bar{q}q)^2}(M^2, \mu) \end{aligned} \quad (7)$$

Sum rules	QCDSR	BFTSR	QCDSR [4]	QCDSR [21]	BFTSR [25]
$m_{f_0(980)}(\text{MeV})$	990 ± 50 (input)		990 ± 50	—	—
$\tilde{f}_{f_0(980)}(\text{MeV})$	335^{+9}_{-12}	331^{+9}_{-12}	370 ± 20	—	—
$m_{f_0(1500)}(\text{MeV})$	—	—	1500 ± 100	[1640, 1730]	[1563, 1706]
$\tilde{f}_{f_0(1500)}(\text{MeV})$	—	—	$-(255 \pm 30)$	[369, 391]	[374, 378]
$M^2(\text{GeV}^2)$	1.6 ± 0.1		[1.1, 1.6]	1.1 ± 0.1	2.0 ± 0.2
$s_0(\text{GeV}^2)$	2.2 ± 0.2		5.0 ± 0.3	6.5 ± 0.3	6.5 ± 0.3

TABLE I. The scalar decay constant of f_0 obtained from QCD sum rules.

with the weighted functions

$$\begin{aligned}
I_0^{\text{pert}}(s_0, M^2) &= \frac{3M^4}{8\pi^2} \left[1 + \frac{\alpha_s(\mu)}{\pi} \left(\frac{17}{3} + 2 \frac{I(1)}{f(1)} - 2 \ln \frac{M^2}{\mu^2} \right) f(1) \right], \\
I_0^{\langle \bar{q}q \rangle}(M^2) &= 3m_q, \quad I_0^{\langle \alpha_s G^2 \rangle}(M^2, \mu) = \frac{1}{8\pi}, \\
I_0^{\langle g_s \bar{q} \sigma T G q \rangle}(M^2) &= -\frac{m_q}{M^2}, \quad I_0^{\langle g_s \bar{q} q \rangle^2}(M^2) = \frac{2\pi\alpha_s}{3M^2}, \quad I_0^{\langle g_s^2 \bar{q} q \rangle^2}(M^2, \mu) = \frac{\pi\alpha_s}{M^2},
\end{aligned} \tag{8}$$

and the functions $I(1) = \int_{e^{-s_0/M^2}}^1 (\ln t) \ln(-\ln t) dt$ and $f(1) = 1 - e^{-s_0/M^2} (1 + s_0/M^2)$. The renormalization group equations of scalar coupling and vacuum condensates are [20, 21]

$$\begin{aligned}
\tilde{f}_S(\mu) &= \tilde{f}_S(\mu_0) L(\mu, \mu_0), \quad m_q(\mu) = m_q(\mu_0) L^{-1}(\mu, \mu_0), \quad \langle \bar{q}q(\mu) \rangle = \langle \bar{q}q(\mu_0) \rangle L(\mu, \mu_0), \\
\langle g_s \bar{q} \sigma T G q(\mu) \rangle &= \langle g_s \bar{q} \sigma T G q(\mu_0) \rangle L^{-1/6}(\mu, \mu_0), \quad \langle g_s \bar{q} q(\mu) \rangle^2 = \langle g_s \bar{q} q(\mu_0) \rangle^2 L(\mu, \mu_0).
\end{aligned} \tag{9}$$

Here $L(\mu, \mu_0) = [\alpha_s(\mu_0)/\alpha_s(\mu)]^{4/b}$. In the numerics, we take $\alpha_s(1 \text{ GeV}) = 0.47$ corresponding to the world average $\alpha_s(m_Z) = 0.118$ and the follow vacuum condensates [22] where the acquiescent scale is 1 GeV.

$$\begin{aligned}
\langle \bar{q}q \rangle &= -0.0156 \text{ GeV}^3, \quad \langle \bar{s}s \rangle = 0.8 \langle \bar{q}q \rangle, \quad \langle \alpha_s G^2 \rangle = 0.012\pi \text{ GeV}^4, \quad m_0^2 = 0.8, \\
\langle g_s \bar{q} \sigma T G q \rangle &= m_0^2 \langle \bar{q}q \rangle, \quad \langle g_s \bar{q} q \rangle^2 = \frac{-16}{9} \langle \bar{q}q \rangle^2, \quad \langle g_s^2 \bar{q} q \rangle^2 = \frac{-16}{3} \langle \bar{q}q \rangle^2.
\end{aligned} \tag{10}$$

The scalar coupling is also studied by the sum rules within the back ground field (BFTSR) [23], where the perturbative term, the quark condensate, dimension-4 gluon condensate and dimension-6 quark-gluon condensate are the same as in the traditional one as shown in Eq. (8), while the dimension-6 four quark condensates are different.

$$I_0^{\langle g_s \bar{q} q \rangle^2}(M^2) = -\frac{8}{27M^2}, \quad I_0^{\langle g_s^2 \bar{q} q \rangle^2}(M^2, \mu) = \frac{2 + \kappa^2}{486\pi^2 M^2} \left[35 + 6 \ln \frac{M^2}{\mu^2} \right]. \tag{11}$$

Meanwhile, the values of the non-perturbative vacuum condensates appearing in the BFTSR are also different from them in the traditional ones.

$$\begin{aligned}
\langle \bar{q}q \rangle &= -0.0242 \text{ GeV}^3, \quad \langle \bar{s}s \rangle = 0.8 \langle \bar{q}q \rangle, \quad \langle \alpha_s G^2 \rangle = 0.038 \text{ GeV}^4, \\
\langle g_s \bar{q} \sigma T G q \rangle &= -0.0193 \text{ GeV}^5, \quad \langle g_s \bar{q} q \rangle^2 = 2.082 \times 10^{-3} \text{ GeV}^6, \\
\langle g_s^2 \bar{q} q \rangle^2 &= 7.420 \times 10^{-3} \text{ GeV}^6, \quad \langle g_s^2 f G^2 \rangle = 0.045 \text{ GeV}^6.
\end{aligned} \tag{12}$$

The Borel mass M^2 is usually chosen by a priori criterion that the contribution from high dimension condensates is no more than twenty percents, and simultaneously the contribution from high excited states and continuum spectral is smaller than thirty percents, so it is a compromise between the unitary interpolation from the hadron summing and the operator production expansion from the QCD calculation. The threshold value s_0 is close to the outset of the first excited state with the same quantum number and determined by the maximal stability of physical quantities once the Borel mass has been set down. Under the statement of $\tilde{f}_\sigma^s = 0$ [24], we consider the f_0 as the ground state with $\bar{s}s$ component in the sum rules Eq. (6) with $q_1 = q_2 = s$. Taking $M^4 \partial / \partial M^2 \ln$ to both sides of Eq. (7), we obtain the sum rules of m_{f_0} which is then fixed at the PDG value $990 \pm 50 \text{ MeV}$. With this input, we ultimately find the optimal choice of Borel mass and threshold value are the same in the two types sum rules of m_{f_0} as shown in Eq. (8) and Eq. (11). This agreement is not a coincidence but a rational result since the only difference between the QCDSR and BFTSR is the expression of terms proportional to dimension-6 four-quark condensate, which is highly power suppressed.

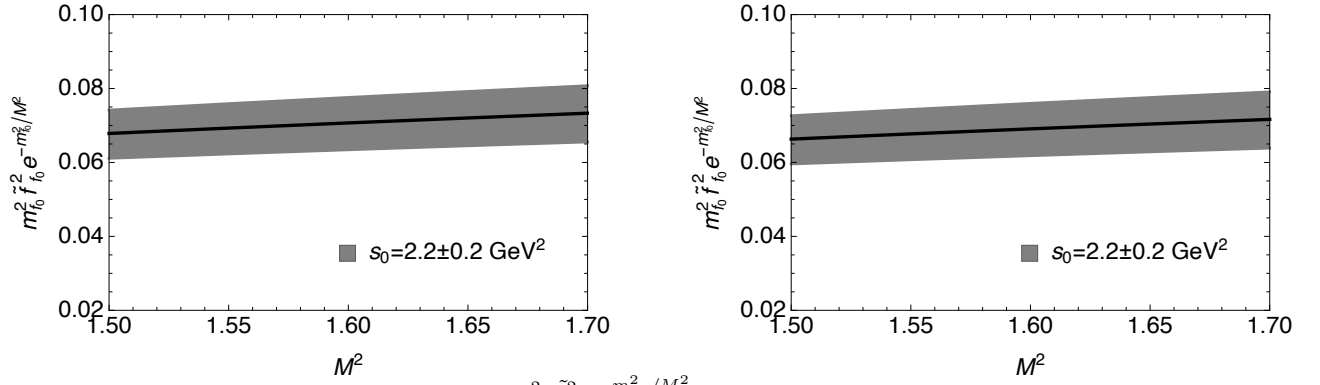


FIG. 1. The Borel mass dependence of $m_{f_0}^2 \tilde{f}_6^2 e^{-m_{f_0}^2/M^2}$ obtained from QCDSR (left) and BFTSR (right).

In table I, we show the sum rules result of scalar decay constant at the default scale 1 GeV. For the sake of comparison, we also present the previous sum rules result [4] where both the ground state f_0 and the first excited state $f_0(1500)$ are taken in to account. The QCDSR is also studied under the statement that $f_0(1500)$ is the ground state with conventional $\bar{s}s$ component while $f_0(980)$ is more like a tetraquark state [21], and the similar BFTSRs study is carried out in Ref. [25]. In figure 1, we show the Borel mass dependence of the sum rules of scalar decay constant as shown in Eq. (7), in which the uncertainty band corresponds to different values of s_0 .

B. Leading twist light-cone distribution amplitudes

The leading twist LCDA is usually expanded in terms of the gegenbauer polynomials

$$\phi(u, \mu) = \bar{f}_S \delta u \bar{u} \sum_{n=0}^{\infty} a_n^{t2}(\mu) C_n^{3/2}(2u-1), \quad (13)$$

from which the multiplicatively renormalization coefficients can be written by

$$a_n(\mu) = \frac{1}{\bar{f}_S} \frac{2(2n+3)}{3(n+1)(n+2)} \int_0^1 C_n^{3/2}(2u-1) \phi(u, \mu) du. \quad (14)$$

Substituting Eq. (13) into the normalization condition in Eq. (3), we obtain $a_{n=\text{even}} \propto 1/\mu_S$ and hence the even coefficients are zero for the neutral scalar mesons. Taking in to account the expansion of gegenbauer polynomials, the renormalization coefficients is rewritten by means of the moments $\langle \zeta_n^q \rangle$

$$\langle \zeta_n^q \rangle = \frac{1}{\bar{f}_S} \int_0^1 (2u-1)^n \phi(u, \mu) du. \quad (15)$$

The first two renormalization coefficients are related to the moments by

$$a_1(\mu) = \frac{5}{3} \langle \zeta_1^q(\mu) \rangle, \quad a_3(\mu) = \frac{21}{4} \langle \zeta_3^q(\mu) \rangle - \frac{9}{4} \langle \zeta_1^q(\mu) \rangle. \quad (16)$$

Here $q = u, d, s$ is the quark component of scalar meson. The renormalization group equation of the gegenbauer coefficients read as

$$a_n(\mu) = a_n(\mu_0) \left[\frac{\alpha_s(\mu_0)}{\alpha_s(\mu)} \right]^{-(\gamma_n^{(0)})/b} L^{-1}(\mu, \mu_0) \quad (17)$$

with the one-loop anomalous dimension

$$\gamma_n^{(0)} = C_F \left[3 + \frac{2}{(n+1)(n+2)} - 4\psi(n+2) - 4\gamma_E \right], \quad (18)$$

in which $b = (11N_c - 2n_f)/3$, $C_F = (N_c^2 - 1)/(2N_c)$.

We consider the correlation function

$$\Pi_n(z, q) = i \int d^4x e^{iq \cdot x} \langle 0 | T \{ \bar{q}_2(x) \not{\epsilon} (iz \cdot \overleftarrow{D})^n q_1(x), \bar{q}_1(0) q_2(0) \} | 0 \rangle. \quad (19)$$

In the deep Euclidean region $q^2 \ll 0$, it can be evaluated directly by applying the OPE technique

$$\begin{aligned} \Pi_n(z, q) = i \int d^4x e^{iq \cdot x} \left\{ -\text{Tr} \cdot \langle 0 | S_0^{q_2}(0, x) \not{\epsilon} (iz \cdot \overleftarrow{D})^n S_0^{q_1}(x, 0) \rangle | 0 \rangle + \langle 0 | \bar{q}_2(x) q_2(0) \not{\epsilon} (iz \cdot \overleftarrow{D})^n S_0^{q_1}(x, 0) \rangle | 0 \rangle \right. \\ \left. + \text{Tr} \cdot \langle 0 | S_0^{q_2}(0, x) \not{\epsilon} (iz \cdot \overleftarrow{D})^n \bar{q}_1(x) q_1(0) \rangle | 0 \rangle + \dots \right\}. \quad (20) \end{aligned}$$

When q^2 shifts from deeply negative to positive, the $\bar{q}q$ state begins to form hadrons and the correlation function can be expressed by the sum of contributions from all possible intermediate states with appropriate subtractions. Writing the hadron representation in the dispersion relation and isolating the ground state contribution, for $q^2 > 0$ we have

$$\Pi_n(z, q) = \frac{1}{\pi} \int_0^\infty ds \frac{\text{Im} \Pi_n^{\text{had}}(s, q^2)}{s - q^2} = \bar{f}_S^2 m_S \langle \zeta_n \rangle + \frac{1}{4\pi^3} \int_{s_0}^\infty ds \frac{3m_q}{(n+2)(s - q^2)}, \quad (21)$$

in which the relationships $\langle 0 | \bar{q}_2 \not{\epsilon} (iz \cdot \overleftarrow{D})^n q_1 | 0 \rangle = (z \cdot q)^{n+1} \bar{f}_S \langle \zeta_n \rangle$ and $\langle 0 | \bar{q}_1 q_2 | S \rangle = m_S \bar{f}_S \langle \zeta_0^s \rangle$ are implied. We take the convention $\langle \zeta_0^s \rangle = 1$ in the following.

After implement the quark-hadron duality and the Borel transformation, the QCDSRs of leading twist LCDA moments ($n = \text{odd}$) is

$$\langle \zeta_n(\mu) \rangle = I_n^{\text{pert}}(s_0, M^2) + \langle \bar{q}q \rangle I_n^{\langle \bar{q}q \rangle}(M^2) + \langle g_s \bar{q} \sigma T G q \rangle I_n^{\langle g_s \bar{q} \sigma T G q \rangle}(M^2) + \langle \alpha_s G^2 \rangle \langle \bar{q}q \rangle I_n^{\langle \alpha_s G^2 \rangle \langle \bar{q}q \rangle}(M^2, \mu). \quad (22)$$

The weighted functions I_n describe the contributions from perturbative and various condensate effects. For the neutral scalar meson $q_1 = q_2 = q$, the result up to dimension six is quoted [4]

$$\begin{aligned} I_n^{\text{pert}}(s_0, M^2) &= -\frac{m_q}{m_S \bar{f}_S^2} e^{m_S^2/M^2} \frac{3M^2}{8\pi^2(n+2)} \left(1 - e^{-s_0/M^2}\right), \\ I_n^{\langle \bar{q}q \rangle}(M^2) &= \frac{2}{m_S \bar{f}_S^2} e^{m_S^2/M^2}, \\ I_n^{\langle g_s \bar{q} \sigma T G q \rangle}(M^2) &= \frac{1}{m_S \bar{f}_S^2} e^{m_S^2/M^2} \frac{10n-3}{12M^2}, \\ I_n^{\langle \alpha_s G^2 \rangle \langle \bar{q}q \rangle}(M^2, \mu) &= \frac{1}{m_S \bar{f}_S^2} e^{m_S^2/M^2} \frac{4\pi n(4n-5)}{18\pi M^4}. \end{aligned} \quad (23)$$

The leading twist LCDA moments are also studied under the BFTSR [23] and the result is

$$\begin{aligned} \langle \zeta_{n=\text{odd}}(\mu) \rangle &= I_n^{\text{pert}}(s_0, M^2) + \langle \bar{q}q \rangle I_n^{\langle \bar{q}q \rangle}(M^2) + \langle g_s \bar{q} \sigma T G q \rangle I_n^{\langle g_s \bar{q} \sigma T G q \rangle}(M^2) + \langle \alpha_s G^2 \rangle I_n^{\langle \alpha_s G^2 \rangle}(M^2, \mu) \\ &+ \langle \alpha_s G^2 \rangle \langle \bar{q}q \rangle I_n^{\langle \alpha_s G^2 \rangle \langle \bar{q}q \rangle}(M^2) + \langle g_s \bar{q}q \rangle^2 I_n^{\langle g_s \bar{q}q \rangle^2}(M^2) + \langle g_s^2 \bar{q}q \rangle^2 I_n^{\langle g_s^2 \bar{q}q \rangle^2}(M^2, \mu) + \langle g_s^3 f G^3 \rangle I_n^{\langle g_s^3 f G^3 \rangle}(M^2, \mu) \end{aligned} \quad (24)$$

The weighted functions associated to the perturbative and quark condensate terms are the same as in the QCDSR. For other nonperturbative condensates with $n \leq 1$, they are

$$\begin{aligned} I_n^{\langle g_s \bar{q} \sigma T G q \rangle}(M^2) &= -\frac{1}{m_S \bar{f}_S^2} e^{m_S^2/M^2} \frac{4n}{3M^2}, \\ I_n^{\langle \alpha_s G^2 \rangle}(M^2, \mu) &= \frac{2m_q}{m_S \bar{f}_S^2} \frac{e^{m_S^2/M^2}}{48\pi M^2} \left\{ -12n \ln \frac{M^2}{\mu^2} - 6(n+2) + \Theta(n-1) \left[-4n \ln \frac{M^2}{\mu^2} + 3\tilde{\psi}(n) - \frac{6}{n} \right] \right\}, \\ I_n^{\langle g_s \bar{q}q \rangle^2}(M^2) &= \frac{m_q}{m_S \bar{f}_S^2} e^{m_S^2/M^2} \frac{4(n+3)}{81M^4}, \\ I_n^{\langle g_s^2 \bar{q}q \rangle^2}(M^2, \mu) &= -\frac{2m_q}{m_S \bar{f}_S^2} e^{m_S^2/M^2} \frac{2 + \kappa^2}{3888\pi^2 M^4} \left\{ 4(n+5) + \delta^{0n} \left[24 \ln \frac{M^2}{\mu^2} - 148 \right] + \delta^{1n} \left[-128 \ln \frac{M^2}{\mu^2} - 692 \right] \right. \\ &\quad \left. + \Theta(n-1) \left[-8(6n^2 + 34n) \ln \frac{M^2}{\mu^2} + 4n\tilde{\psi}(n) - 2(6n^2 + 96n + 212) \right] \right\}, \\ I_n^{\langle g_s^3 f G^3 \rangle}(M^2, \mu) &= -\frac{2m_q}{m_S \bar{f}_S^2} e^{m_S^2/M^2} \frac{1}{384\pi^2 M^4} \left\{ \delta^{1n} \left[24 \ln \frac{M^2}{\mu^2} + 84 \right] \right. \\ &\quad \left. + \Theta(n-1) \left[4n(3n-5) \ln \frac{M^2}{\mu^2} + 2(2n^2 + 5n - 13) \right] \right\}. \end{aligned} \quad (25)$$

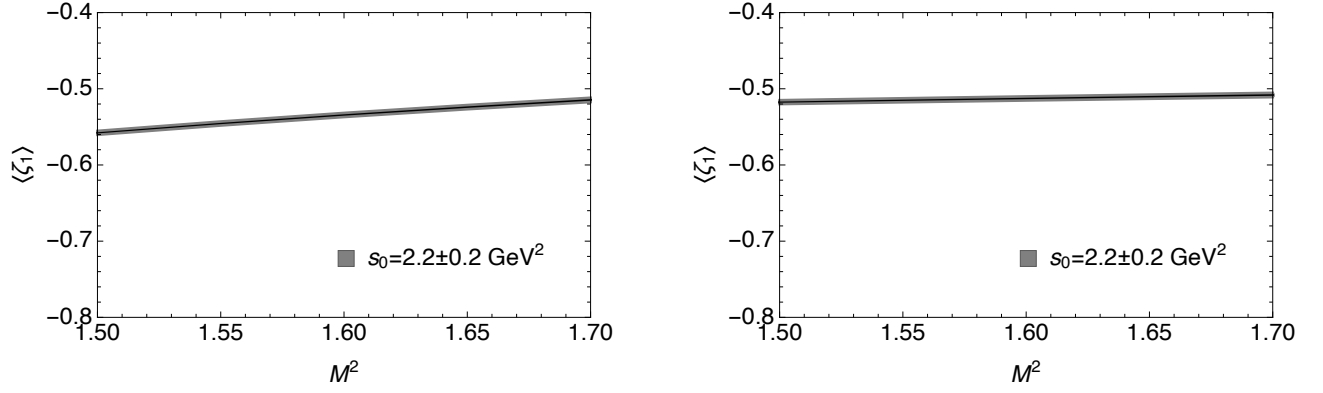


FIG. 2. The Borel mass dependence of the first moment obtained from the QCDSR (left) and BFTSR (right).

Sum rules	QCDSR	BFTSR	QCDSR [4]	QCDSR [26]	BFTSR [23]
$a_1(f_0(980))$	$-0.891^{+0.039+0.004}_{-0.033-0.004}$	$-0.855^{+0.039+0.004}_{-0.033-0.005}$	-0.78 ± 0.08	—	-0.51 ± 0.07
$a_1(f_0(1500))$	—	—	0.80 ± 0.40	-0.48 ± 0.11	—
$M^2(\text{GeV}^2)$	1.6 ± 0.1	—	[1.1, 1.6]	—	[2.5, 3.5]
$s_0(\text{GeV}^2)$	2.2 ± 0.2	—	5.0 ± 0.3	—	7.0

TABLE II. The first gegenbauer coefficients obtained from QCD sum rules.

Here $\tilde{\psi}(n) = \psi((n+1)/2) - \psi(n/2) + (-1)^n \ln 4$, $\psi(n+2) = \sum_{j=1}^{n+1} 1/j - \gamma_E$, $\kappa = 0.74 \pm 0.03$.

In figure 2 we show the Borel mass dependence of the first moment obtained from sum rules. Because the moments are dominated by the nonperturbative contributions, we see that $\langle \zeta_1 \rangle$ is not sensitive to the threshold value s_0 . In table II we show the result of the first gegenbauer coefficient, where the first and second errors arise from M^2 and s_0 , respectively. For the sake of comparison, we also present the result obtained from previous sum rules¹. Our result of the first gegenbauer coefficient a_1 obtained from the QCDSR is consistent with the previous sum rules determination [4], the result is almost the same as that obtained from the BFTSR with the same sum rules parameters.

C. Subleading twist light-cone distribution amplitudes

Twist three light-cone distribution amplitudes associated with two particle composition are expanded also in terms of gegenbauer polynomials [26]

$$\begin{aligned} \phi^s(u, \mu) &= \bar{f}_S \left[1 + \sum_{n=1}^{\infty} a_n^s(\mu) C_n^{1/2}(2u-1) \right], \\ \phi^\sigma(u, \mu) &= \bar{f}_S 6u\bar{u} \left[1 + \sum_{n=1}^{\infty} a_n^\sigma(\mu) C_n^{3/2}(2u-1) \right]. \end{aligned} \quad (26)$$

The scalar and tensor moments defined in

$$\langle \zeta_n^{s/\sigma} \rangle = \int_0^1 du (2u-1)^n \phi^{s/\sigma}(u, \mu) \quad (27)$$

relate to the gegenbauer coefficients $a_n^{s/\sigma}$ by

$$\begin{aligned} a_1^s &= 3\langle \zeta_1^s \rangle, & a_2^s &= \frac{5}{2} [3\langle \zeta_2^s \rangle - 1], & a_4^s &= \frac{9}{8} [35\langle \zeta_4^s \rangle - 30\langle \zeta_2^s \rangle + 3], \\ a_1^\sigma &= \frac{5}{3}\langle \zeta_1^\sigma \rangle, & a_2^\sigma &= \frac{7}{12} [5\langle \zeta_2^\sigma \rangle - 1], & a_4^\sigma &= \frac{11}{24} [21\langle \zeta_4^\sigma \rangle - 14\langle \zeta_2^\sigma \rangle + 1]. \end{aligned} \quad (28)$$

¹ In the last column, we take the SU(3) asymptotic and compare directly to the result obtained for the isovector scalar meson $a_0(980)$ [25].

We consider two correlation functions

$$\Pi_n^s(z, q) = i \int d^4x e^{iq \cdot x} \langle 0 | T \left\{ \bar{q}_2(x) \left(iz \cdot \overleftrightarrow{D} \right)^n q_1(x), \bar{q}_1(0) q_2(0) \right\} | 0 \rangle = - (z \cdot q)^n I_n(q^2), \quad (29)$$

$$\Pi_n^\sigma(z, q) = i \int d^4x e^{iq \cdot x} \langle 0 | T \left\{ \bar{q}_2(x) \sigma_{\mu\nu} \left(iz \cdot \overleftrightarrow{D} \right)^n q_1(x), \bar{q}_1(0) q_2(0) \right\} | 0 \rangle = i (q_\mu z_\nu - q_\nu z_\mu) (z \cdot q)^n I_n^\sigma(q^2). \quad (30)$$

The dispersion relation representation of the correlation functions in the physical regions reads as

$$\Pi_n^{s/\sigma}(z, q) = \frac{1}{\pi} \int ds \frac{\text{Im} \Pi_n^{s/\sigma, \text{had}}(s, q^2)}{s - q^2}. \quad (31)$$

With the definitions of local matrix elements in terms of moments

$$\begin{aligned} \langle 0 | \bar{q}_2(x) \left(iz \cdot \overleftrightarrow{D} \right)^n q_1(x) | S(q) \rangle &= m_S \bar{f}_S (q \cdot z)^n \langle \zeta_n^s \rangle, \\ \langle 0 | \bar{q}_2(x) \sigma_{\mu\nu} \left(iz \cdot \overleftrightarrow{D} \right)^{n+1} q_1(x) | S(q) \rangle &= -i \frac{n+1}{3} m_S \bar{f}_S (q_\mu z_\nu - q_\nu z_\mu) (q \cdot z)^n \langle \zeta_n^\sigma \rangle, \end{aligned} \quad (32)$$

we obtain the imaginary parts for the neutral scalar mesons²,

$$\begin{aligned} \frac{1}{\pi} \text{Im} I_{n=\text{even}}^{s, \text{had}} &= -\delta(q^2 - m_S^2) m_S^2 \bar{f}_S^2 \langle \zeta_{n=\text{even}}^s \rangle + \Theta(q^2 - s_0^s) \frac{3(-q^2 + 4m_q^2)}{8\pi^2} \frac{1}{n+1}, \\ \frac{1}{\pi} \text{Im} I_{n=\text{even}}^{\sigma, \text{had}} &= -\delta(q^2 - m_S^2) m_S^2 \bar{f}_S^2 \langle \zeta_{n=\text{even}}^\sigma \rangle \frac{n+1}{3} + \Theta(q^2 - s_0^s) \frac{3(-q^2 + 2m_q^2)}{8\pi^2} \frac{1}{n+3}. \end{aligned} \quad (33)$$

In the deep Euclidean region, the correlation functions can be evaluated using operator product expansion at quark level. After applying the quark-hadron duality to math the result of $I_n^{s/\sigma}(q^2)$ obtained from the hadron interpolating and OPE calculation, for the neutral scalar mesons, the Borelization result of the second moments are [21]

$$\begin{aligned} -m_S^2 \bar{f}_S^2 e^{-m_S^2/M^2} \langle \zeta_{n=\text{even}}^s \rangle &= -\frac{3}{8\pi^2} \frac{1}{n+1} \int_0^{s_0^s} s e^{-s/M^2} ds - \langle \alpha_s G^2 \rangle \frac{1}{8\pi} - \langle \bar{q}q \rangle (n+3) m_q \\ &+ \langle g_s \bar{q} \sigma T G q \rangle \frac{(4n^2 + 23n + 12) m_q}{12} \frac{1}{M^2} + 4\pi \alpha_s \langle \bar{q}q \rangle^2 \frac{(-8n^2 + 16n + 150)}{81} \frac{1}{M^2}, \end{aligned} \quad (34)$$

$$\begin{aligned} -\frac{1}{3} m_S^2 \bar{f}_S^2 e^{-m_S^2/M^2} \langle \zeta_{n=\text{even}}^\sigma \rangle &= -\frac{3}{8\pi^2} \frac{1}{(n+1)(n+3)} \int_0^{s_0^s} s e^{-s/M^2} ds - \langle \alpha_s G^2 \rangle \frac{1}{24\pi} \frac{1}{n+1} - \langle \bar{q}q \rangle m_q \\ &+ \frac{1}{n+1} \frac{1}{M^2} \left\{ \langle g_s \bar{q} \sigma T G q \rangle \frac{(4n^2 + 7n + 5) m_q}{12} - 4\pi \alpha_s \langle \bar{q}q \rangle^2 \left[\frac{8n^2 + 9n - 35}{162} + \frac{2\delta_{n0}}{9} \right] \right\}, \end{aligned} \quad (35)$$

Besides the QCDSR result, the BFTSR also applied to calculate the scalar and tensor moments with the accuracy up to the linear terms of quark mass contributions [25].

$$\begin{aligned} -m_S^2 \bar{f}_S^2 e^{-m_S^2/M^2} \langle \zeta_{n=\text{even}}^s \rangle &= -\frac{3}{8\pi^2} \frac{1}{n+1} M^4 + \frac{3}{8\pi^2} \frac{e^{-s_0^s/M^2}}{n+1} [M^4 + s_0^s M^2 - 2(n+2) m_q^2 M^2] \\ &- \langle \alpha_s G^2 \rangle \frac{1}{8\pi} - \langle \bar{q}q \rangle (n+3) m_q + \langle g_s^3 f G^3 \rangle \frac{n}{96\pi^2} \frac{1}{M^2} \\ &+ \langle g_s \bar{q} \sigma T G q \rangle \frac{(8n^2 + 13n - 18) m_q}{18} \frac{1}{M^2} + 4\pi \alpha_s \langle \bar{q}q \rangle^2 \frac{(-4n^2 - 14n + 168)}{81} \frac{1}{M^2}, \end{aligned} \quad (36)$$

$$\begin{aligned} -\frac{1}{3} m_S^2 \bar{f}_S^2 e^{-m_S^2/M^2} \langle \zeta_{n=\text{even}}^\sigma \rangle &= \frac{3}{8\pi^2} \frac{1}{(n+1)(n+3)} M^4 - \frac{3}{8\pi^2} \frac{e^{-s_0^s/M^2}}{(n+1)(n+3)} [M^4 + s_0^s M^2 - 2(n+3) m_q^2 M^2] \\ &- \langle \alpha_s G^2 \rangle \frac{1}{24\pi} \frac{1}{n+1} - \langle \bar{q}q \rangle m_q + \langle g_s \bar{q} \sigma T G q \rangle \frac{(8n+7) m_q}{18} \frac{1}{M^2} + 4\pi \alpha_s \langle \bar{q}q \rangle^2 \frac{(-4n+10)}{81} \frac{1}{M^2}. \end{aligned} \quad (37)$$

² We here concentrate on the correlation functions with even n since the odd ones result to zero moments for the neutral meson due to the C -parity conservation.

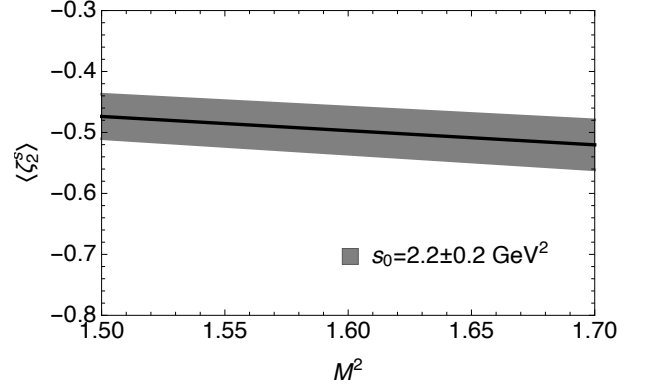
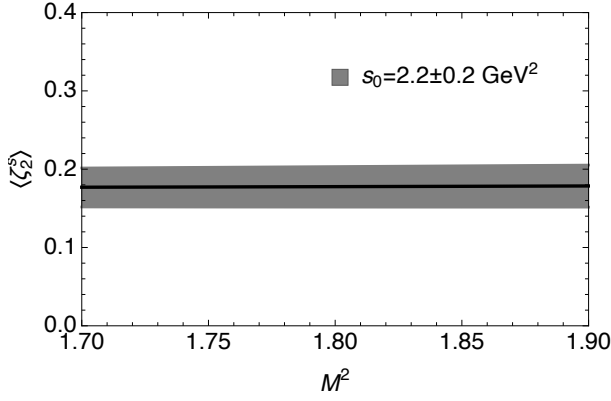


FIG. 3. The Borel mass dependence of the $\langle \zeta_2^s \rangle$ obtained from the QCDSR (left) and BFTSR (right).

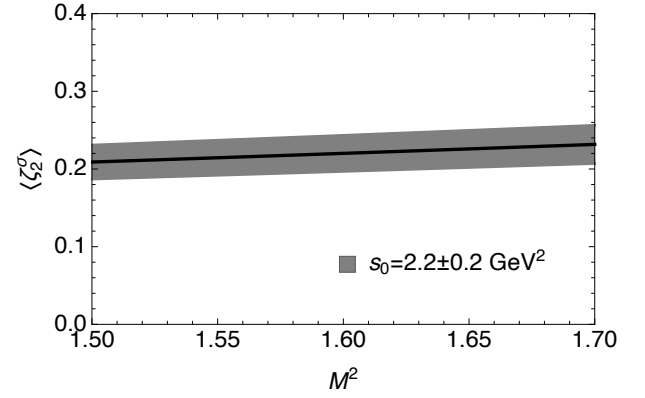
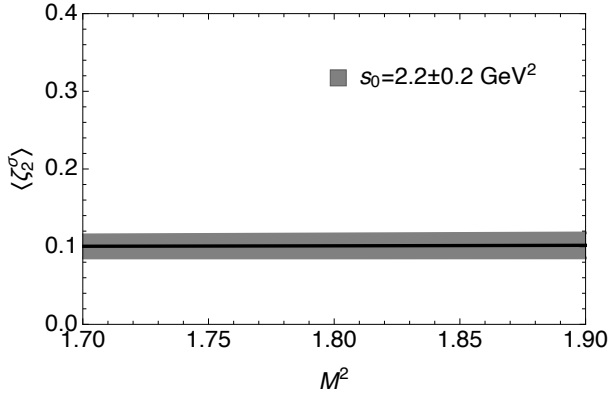


FIG. 4. The same as figure 3, but for the second tensor moment $\langle \zeta_2^\sigma \rangle$.

Figure 3 and figure 4 show the Borel mass dependence of the second scalar and tensor moments. Its easy to find the apparent difference between the result obtained from QCDSR and BFTSR, and hence the different predictions for the gegenbauer coefficients as shown in table III and table IV.

Twist three LCDAs also contributed from three particle composition [27–29]

$$\phi_{3S}^q(p_1, \alpha_i) = 360 f_{3S} \alpha_1 \alpha_2 \alpha_3^2 [1 + \lambda_{3S} (\alpha_1 - \alpha_2) + \omega_{3S} (7\alpha_3 - 3)]. \quad (38)$$

where the nonperturbative parameters is defined by the local matrix elements

$$\begin{aligned} \langle S(p_1) | \bar{q}_2(z) g_s G \cdot \sigma q_1(z) | 0 \rangle &= 2 f_{3S} (p_1 \cdot z)^2, \\ \langle S(p_1) | \bar{q}_2(z) \overleftrightarrow{D} g_s G \cdot \sigma q_1(z) - \bar{q}_2(z) g_s G \cdot \sigma \overleftrightarrow{D} q_1(z) | 0 \rangle &= -2 f_{3S} \lambda_{3S} (p_1 \cdot z)^3 / 14, \\ \langle S(p_1) | \bar{q}_2(z) \sigma^{\mu\nu} [iD, g_s G_{\mu\nu}] q_1(z) - \frac{3}{7} \partial \bar{q}_2(z) g_s G \cdot \sigma \overleftrightarrow{D} q_1(z) | 0 \rangle &= -f_{3S} \omega_{3S} (p_1 \cdot z)^3 / 14. \end{aligned} \quad (39)$$

The renormalization group equations of them are

$$\begin{aligned} f_{3S}(\mu) &= f_{3S}(\mu_0) L(\mu, \mu_0)^{-\gamma_{f_{3S}}/8}, \\ [f_{3S} \lambda_{3S}](\mu) &= [f_{3S} \lambda_{3S}](\mu_0) L(\mu, \mu_0)^{-\gamma_{\lambda_{3S}}/8}, \\ [f_{3S} \omega_{3S}](\mu) &= [f_{3S} \omega_{3S}](\mu_0) L(\mu, \mu_0)^{-\gamma_{\omega_{3S}}/8}, \end{aligned} \quad (40)$$

at one loop accuracy, the anomalous dimensions are

$$\gamma_{f_{3S}}^{(0)} = \frac{110}{9}, \quad \gamma_{\lambda_{3S}}^{(0)} = \frac{139}{9}, \quad \gamma_{\omega_{3S}}^{(0)} = \frac{208}{9}. \quad (41)$$

In the numerics we take $\lambda_{3f_0} = 0$ due to the G -odd definition, and $\omega_{3f_0}(1\text{GeV}) = -1.5 \pm 0.7$ as the same as $\omega_{3\pi}$. The

Sum rules	QCDSR	BFTSR	QCDSR [21]	BFTSR [25]
$a_2^s(f_0(980))$	0.296 ± 0.044	-0.828 ± 0.065	—	—
$a_2^s(f_0(1500))$	—	—	$[-0.33, -0.18]$	$[-0.02, 0.05]$
$M^2(\text{GeV}^2)$	1.8 ± 0.1	1.6 ± 0.1	1.7 ± 0.2	2.0 ± 0.2
$s_0(\text{GeV}^2)$	2.2 ± 0.2		6.5 ± 0.3	6.5 ± 0.3

TABLE III. The second gegenbauer coefficients obtained from the scalar sum rules.

Sum rules	QCDSR	BFTSR	QCDSR [21]	BFTSR [25]
$a_2^\sigma(f_0(980))$	0.169 ± 0.026	0.367 ± 0.039	—	—
$a_2^\sigma(f_0(1500))$	—	—	$[-0.15, -0.09]$	$[-0.03, 0.00]$
$M^2(\text{GeV}^2)$	1.8 ± 0.1	1.6 ± 0.1	1.65 ± 0.15	2.0 ± 0.2
$s_0(\text{GeV}^2)$	2.2 ± 0.2		6.5 ± 0.3	6.5 ± 0.3

TABLE IV. The second gegenbauer coefficients obtained from the tensor sum rules.

additional scalar coupling is related to the gegenbauer moments $\langle \zeta_{n=0,2}^{s/\sigma} \rangle$ and \bar{f}_{f_0} by by the equation of motion

$$\langle \zeta_2^s \rangle = \frac{1}{3} \langle \zeta_0^s \rangle + \frac{4}{m_{f_0}} \frac{\bar{f}_{3f_0}}{\bar{f}_{f_0}}, \quad \langle \zeta_2^\sigma \rangle = \frac{1}{5} \langle \zeta_0^\sigma \rangle + \frac{12}{5m_{f_0}} \frac{\bar{f}_{3f_0}}{\bar{f}_{f_0}} - \frac{8}{5m_{f_0}} \frac{\bar{f}_{3f_0}}{\bar{f}_{f_0}} \langle \langle \alpha_3 \rangle \rangle_{f_0}. \quad (42)$$

The moments of three particle distribution amplitudes are defined

$$\langle \langle (\alpha_2 - \alpha_1 + v\alpha_3)^n \rangle \rangle = \int \mathcal{D}\alpha_i \phi_{3S}(\alpha_i) (\alpha_2 - \alpha_1 + v\alpha_3)^n. \quad (43)$$

III. $D_s \rightarrow f_0$ FORM FACTORS

$D_s \rightarrow f_0$ transition form factors are defined by

$$\begin{aligned} \langle f_0(p_1) | \bar{s} \gamma_\mu \gamma_5 c | D_s^+(p) \rangle &= -i f_1(q^2) \left[(p + p_1)_\mu - \frac{m_{D_s}^2 - m_{f_0}^2}{q^2} q_\mu \right] - i f_0(q^2) \frac{m_{D_s}^2 - m_{f_0}^2}{q^2} q_\mu \\ &= -i \left[f_+(q^2) (p + p_1)_\mu + f_-(q^2) q_\mu \right]. \\ \langle f_0(p_1) | \bar{s} \sigma_{\mu\nu} \gamma_5 q^\mu c | D_s^+(p) \rangle &= -\frac{f_T(q^2)}{m_{D_s} + m_{f_0}} \left[q^2 (p + p_1)_\nu - (m_{D_s}^2 - m_{f_0}^2) q_\nu \right]. \end{aligned} \quad (44)$$

Here $q = p - p_1$ is the transfer momentum, the relations between two definitions are

$$f_+(q^2) = f_1(q^2), \quad f_-(q^2) = \frac{m_{D_s}^2 - m_{f_0}^2}{q^2} f_0(q^2) - \frac{m_{D_s}^2 - m_{f_0}^2}{q^2} f_1(q^2). \quad (45)$$

To evaluate the $D_s \rightarrow f_0$ form factors, we start with the correlation functions

$$\Pi_\mu^{S_i}(p_1, q) = i \int d^4x e^{iqx} \langle f_0(p_1) | T \{ j_{1,\mu}^{S_i}(x), j_2^{S_i} \} | 0 \rangle, \quad (46)$$

$$\tilde{\Pi}_\mu^{S_i}(p_1, q) = i \int d^4x e^{iqx} \langle f_0(p_1) | T \{ \tilde{j}_{1,\mu}^{S_i}(x), j_2^{S_i} \} | 0 \rangle, \quad (47)$$

where $j_{1,\mu}$ and $\tilde{j}_{1,\mu}$ are the weak transition currents, j_2 is the hadron interpolating current. Roman alphabets S_i denote different scenarios of the currents as shown in table III. We highlight that both the leading and subleading twist LCDAs of scalar meson contribute to $D_s \rightarrow f_0$ form factors if we take the conventional non-chiral currents, while only the leading or subleading twist LCDAs contribute to the form factors if we take the chiral currents.

In the physical region, the long-distance quark-gluon interaction between the two currents in Eqs. (46,47) begins to form hadrons. In this respect, the correlation function can be understood by the sum of contributions from all possible intermediate

Scenarios	$j_{1,\mu}^{S_1}$	$\tilde{j}_{1,\mu}^{S_1}$	$j_2^{S_1}$	f_+, f_-, f_T
S ₁	$\bar{s}\gamma_\mu\gamma_5 c$	$\bar{s}\sigma_{\mu\nu}\gamma_5 q^\nu c$	$\bar{c}i\gamma_5 s$	$\phi, \phi^s, \phi^\sigma$
S ₂	$\bar{s}\gamma_\mu(1-\gamma_5)c$	$\bar{s}\sigma_{\mu\nu}(1+\gamma_5)q^\nu c$	$\bar{c}i(1-\gamma_5)s$	ϕ
S ₃	$\bar{s}\gamma_\mu(1-\gamma_5)c$	$\bar{s}\sigma_{\mu\nu}(1+\gamma_5)q^\nu c$	$\bar{c}i(1+\gamma_5)s$	ϕ^s, ϕ^σ

TABLE V. Scenarios of the currents to evaluate the $D_s \rightarrow f_0$ form factors.

states with appropriate subtractions. We take the (axial)-vector current in the weak vertex for example to show the dispersion relation of invariant amplitudes in variable $(p_1 + q)^2 > 0$, which is written in

$$\Pi_\mu^{S_1, \text{had}}(p_1, q) = \frac{\langle f_0(p_1) | j_{1,\mu}^{S_1}(x) | D_s(p_1 + q) \rangle \langle D_s | j_s^{S_1}(0) | 0 \rangle}{m_{D_s}^2 - (p_1 + q)^2} + \frac{1}{\pi} \int_{s_0^i}^\infty ds \frac{\rho_\mu^h(s, q^2)}{s - (p_1 + q)^2}. \quad (48)$$

The ground state D_s is isolated from the contributions from excited states and continuum spectra by introducing a threshold value s_0 . With the form factors defined in Eqs. (44) and the decay constant defined as $\langle D_s(p_1 + q) | j_s^{S_1}(0) | 0 \rangle = m_{D_s}^2 f_{D_s} / (m_c + m_s)$, the hadron representation is rewritten as

$$\Pi_\mu^{S_1, \text{had}}(p_1, q) = \frac{-im_{D_s}^2 f_{D_s} [2f_+(q^2)p_{1\nu} + (f_+(q^2) + f_-(q^2))q_\mu]}{(m_c + m_s) [m_{D_s}^2 - (p_1 + q)^2]} + \frac{1}{\pi} \int_{s_0^1}^\infty ds \frac{\rho_+^h(s, q^2)p_{1\mu} + \rho_-^h(s, q^2)q_\mu}{s - (p_1 + q)^2}. \quad (49)$$

The relations between different scenarios read as

$$\Pi_\mu^{S_1, \text{had}}(p_1, q) = \Pi_\mu^{S_2, \text{had}}(p_1, q) = -\Pi_\mu^{S_3}(p_1, q). \quad (50)$$

In the Euclidean momenta space with negative q^2 , the correlation functions can be evaluated directly by QCD at the quark-gluon level. Since the operator product expansion (OPE) is valid for large energies of the final state vector mesons, the momentum transfer squared is restriction to be not too large $0 \leq |q^2| \leq q_{\text{max}}^2$, and hence the operator product of the c -quark fields in the correlation function can be expanded near the light cone $x^2 \sim 0$ due to the large virtuality,

$$S_c(x, 0, m_c) \equiv -i \langle 0 | T \{ c_i(x), \bar{c}_j(0) \} | 0 \rangle = -i \frac{m_c^2}{4\pi^2} \left[\frac{K_1(m_c \sqrt{|x^2|})}{\sqrt{|x^2|}} + \frac{i \not{x} K_2(m_c \sqrt{|x^2|})}{|x^2|} \right] \delta_{ij} \\ - i \frac{gm_c}{16\pi^2} \int_0^1 du \left[G \cdot \sigma K_0(m_c \sqrt{|x^2|}) + i \frac{[\bar{u} \not{x} G \cdot \sigma + u G \cdot \sigma \not{x}] K_1(m_c \sqrt{|x^2|})}{\sqrt{|x^2|}} \right] \delta_{ij} + \dots \quad (51)$$

The first term corresponds to the free charm quark propagator, the second one corresponds to the quark-gluon interaction at leading power, and the ellipsis denotes the high power corrections from the quark-gluon interaction. $\bar{u} = 1 - u$ is indicated. The correlation functions are ultimately written in a general convolution of hard functions with various LCDAs at different twists

$$\Pi_\mu^{S_i, \text{OPE}}(p_1, q) = \sum_t \int_0^1 du T_\mu^{(t)}(u, q^2, (p_1 + q)^2) \otimes \phi^{(t)}(u) + \int_0^1 du \int_0^u \mathcal{D}\alpha_i T'_\mu(u, \alpha_i, q^2, (p_1 + q)^2) \otimes \phi_{3f_0}(\alpha_i), \quad (52)$$

where the first term comes from the two particle LCDAs, and the second term comes from the twist three LCDA with three particle configuration. The OPE amplitudes in Eq. (52) can also be written in a dispersion integral over the invariant mass of the interpolating heavy meson

$$\Pi_\mu^{S_i, \text{OPE}}(p_1, q) = \frac{1}{\pi} \int_0^1 du \sum_{n=1,2} \left[\frac{\text{Im}\Pi_{+,n}^{S_i, \text{OPE}}(q^2, u) p_{1\mu} + \text{Im}\Pi_{-,n}^{S_i, \text{OPE}}(q^2, u) q_\mu}{u^n [s_2(u) - (p_1 + q)^2]^n} \right. \\ \left. + \int_0^u \mathcal{D}\alpha_i \frac{\text{Im}\Pi_{+,n}^{S_i, \text{OPE}}(q^2, u, \alpha_i) p_{1\mu} + \text{Im}\Pi_{-,n}^{S_i, \text{OPE}}(q^2, u, \alpha_i) q_\mu}{[\alpha_2 + v(1 - \alpha_1 - \alpha_2)]^n [s_3(u, \alpha_i) - (p_1 + q)^2]^n} \right]. \quad (53)$$

Here the momentum fraction dependent kinematical variables read as $s_2(u) = \bar{u}m_{f_0}^2 + (m_c^2 - \bar{u}q^2)/u$ and $s_3(u, \alpha_i) = (1 - \alpha_2 - v\alpha_3)m_{f_0}^2 + [m_c^2 - (1 - \alpha_2 - v\alpha_3)q^2]/(\alpha_2 + v\alpha_3)$.

We then implement the quark-hadron duality to eliminate the contribution from the excited and continuum spectra with the threshold invariant mass s_0^j . In order to improve the reliability of quark-hadron duality, we Borel transfer both the hadronic

representation and the OPE evaluation of the correlation functions. This operation, from one hand, sticks out the ground scalar meson by suppressing the contribution from the excited and continuum spectra in the hadron representation, from the other hand, is helpful to obtain the convergent power expansion in the OPE evaluation. The $D_s \rightarrow f_0$ form factors obtained from LCSRs approach with different currents are collected as follow,

$$\begin{aligned}
f_+^{S1}(q^2) &= \frac{m_c + m_s}{2m_{D_s}^2 f_{D_s}} \left\{ \int_{u_0}^1 \frac{du}{u} \left[-m_c \phi(u) + um_{f_0} \phi^s(u) + \frac{m_{f_0} \phi^\sigma(u)}{3} + \frac{m_{f_0} \phi^\sigma(u)}{6} \frac{m_c^2 + q^2 - u^2 m_{f_0}^2}{uM^2} \right] e^{-\frac{-s_2(u) + m_{D_s}^2}{M^2}} \right. \\
&+ \int_{u_0}^1 du \int_0^u d\alpha_1 \int_0^{1-u} \frac{d\alpha_2}{\alpha_3} \frac{8m_{f_0}^2 f_{3f_0}^s \phi_{3f_0}^s(\alpha_i)}{[\alpha_2 + v\alpha_3] M^2} e^{-\frac{-s_3(u, \alpha_i) + m_{D_s}^2}{M^2}} + \frac{m_{f_0} \phi^\sigma(u_0)}{6} \frac{m_c^2 + q^2 - u_0^2 m_{f_0}^2}{m_c^2 - q^2 + u_0^2 m_{f_0}^2} e^{-\frac{-s_0^1 + m_{D_s}^2}{M^2}} \\
&\left. + \int_0^{u_0} d\alpha_1 \int_0^{1-u_0} \frac{d\alpha_2}{\alpha_3} \frac{8m_{f_0}^2 f_{3f_0}^s \phi_{3f_0}^s(\alpha_i) (\alpha_2 + v_0 \alpha_3)}{[m_c^2 - q^2 + (\alpha_2 + v_0 \alpha_3)^2 m_{f_0}^2]} e^{-\frac{-s_0^1 + m_{D_s}^2}{M^2}} \right\}, \quad (54)
\end{aligned}$$

$$\begin{aligned}
f_+^{S1}(q^2) + f_-^{S1}(q^2) &= \frac{m_c + m_s}{m_{D_s}^2 f_{D_s}} \left\{ \int_{u_0}^1 \frac{du}{u} \left[m_{f_0} \phi^s(u) + \frac{m_{f_0} \phi^\sigma(u)}{6u} - \frac{m_{f_0} \phi^\sigma(u)}{6} \frac{m_c^2 - q^2 + u^2 m_{f_0}^2}{u^2 M^2} \right] e^{-\frac{-s_2(u) + m_{D_s}^2}{M^2}} \right. \\
&+ \int_{u_0}^1 du \int_0^u d\alpha_1 \int_0^{1-u} \frac{d\alpha_2}{\alpha_3} \frac{8m_{f_0}^2 f_{3f_0}^s \phi_{3f_0}^s(\alpha_i)}{[\alpha_2 + v\alpha_3]^2 M^2} e^{-\frac{-s_3(u, \alpha_i) + m_{D_s}^2}{M^2}} - \frac{m_{f_0} \phi^\sigma(u_0)}{6u_0} e^{-\frac{-s_0^1 + m_{D_s}^2}{M^2}} \\
&\left. + \int_0^{u_0} d\alpha_1 \int_0^{1-u_0} \frac{d\alpha_2}{\alpha_3} \frac{8m_{f_0}^2 f_{3f_0}^s \phi_{3f_0}^s(\alpha_i)}{[m_c^2 - q^2 + (\alpha_2 + v_0 \alpha_3)^2 m_{f_0}^2]} e^{-\frac{-s_0^1 + m_{D_s}^2}{M^2}} \right\}, \quad (55)
\end{aligned}$$

$$\begin{aligned}
f_T^{S1}(q^2) &= \frac{(m_c + m_s)(m_{D_s} + m_{f_0})}{m_{D_s}^2 f_{D_s}} \left\{ \int_{u_0}^1 \frac{du}{u} \left[-\frac{\phi(u)}{2} + \frac{m_{f_0} \phi^\sigma(u)}{6} \frac{m_c}{uM^2} \right] e^{-\frac{-s_2(u) + m_{D_s}^2}{M^2}} \right. \\
&\left. + \frac{m_{f_0} \phi^\sigma(u_0)}{6} \frac{m_c}{[m_c^2 - q^2 + u_0^2 m_{f_0}^2]} e^{-\frac{-s_0^1 + m_{D_s}^2}{M^2}} \right\}, \quad (56)
\end{aligned}$$

$$f_+^{S2}(q^2) = -\frac{m_c(m_c + m_s)}{m_{D_s}^2 f_{D_s}} \int_{u_0}^1 \frac{du}{u} \phi(u) e^{-\frac{-s_2(u) + m_{D_s}^2}{M^2}}, \quad (57)$$

$$f_+^{S2}(q^2) + f_-^{S2}(q^2) = 0, \quad (58)$$

$$f_T^{S2}(q^2) = -\frac{(m_c + m_s)(m_{D_s} + m_{f_0})}{m_{D_s}^2 f_{D_s}} \int_{u_0}^1 \frac{du}{u} \phi(u) e^{-\frac{-s_2(u) + m_{D_s}^2}{M^2}}, \quad (59)$$

$$\begin{aligned}
f_+^{S3}(q^2) &= \frac{(m_c + m_s) m_{f_0}}{2m_{D_s}^2 f_{D_s}} \left\{ \int_{u_0}^1 \frac{du}{u} \left[2u\phi^s(u) + \frac{2\phi^\sigma(u)}{3} + \frac{\phi^\sigma(u)}{3} \frac{m_c^2 + q^2 - u^2 m_{f_0}^2}{uM^2} \right] e^{-\frac{-s_2(u) + m_{D_s}^2}{M^2}} \right. \\
&+ \int_{u_0}^1 du \int_0^u d\alpha_1 \int_0^{1-u} \frac{d\alpha_2}{\alpha_3} \frac{16m_{f_0} f_{3f_0}^s \phi_{3f_0}^s(\alpha_i)}{[\alpha_2 + v\alpha_3] M^2} e^{-\frac{-s_3(u, \alpha_i) + m_{D_s}^2}{M^2}} + \frac{\phi^\sigma(u_0)}{3} \frac{m_c^2 + q^2 - u_0^2 m_{f_0}^2}{m_c^2 - q^2 + u_0^2 m_{f_0}^2} e^{-\frac{-s_0^1 + m_{D_s}^2}{M^2}} \\
&\left. + \int_0^{u_0} d\alpha_1 \int_0^{1-u_0} \frac{d\alpha_2}{\alpha_3} \frac{16m_{f_0} f_{3f_0}^s \phi_{3f_0}^s(\alpha_i) (\alpha_2 + v_0 \alpha_3)}{[m_c^2 - q^2 + (\alpha_2 + v_0 \alpha_3)^2 m_{f_0}^2]} e^{-\frac{-s_0^1 + m_{D_s}^2}{M^2}} \right\}, \quad (60)
\end{aligned}$$

$$\begin{aligned}
f_+^{S3}(q^2) + f_-^{S3}(q^2) &= \frac{(m_c + m_s) m_{f_0}}{m_{D_s}^2 f_{D_s}} \left\{ \int_{u_0}^1 \frac{du}{u} \left[2\phi^s(u) + \frac{\phi^\sigma(u)}{3u} - \frac{\phi^\sigma(u)}{3} \frac{m_c^2 - q^2 + u^2 m_{f_0}^2}{u^2 M^2} \right] e^{-\frac{-s_2(u) + m_{D_s}^2}{M^2}} \right. \\
&+ \int_{u_0}^1 du \int_0^u d\alpha_1 \int_0^{1-u} \frac{d\alpha_2}{\alpha_3} \frac{16m_{f_0} f_{3f_0}^s \phi_{3f_0}^s(\alpha_i)}{[\alpha_2 + v\alpha_3]^2 M^2} e^{-\frac{-s_3(u, \alpha_i) + m_{D_s}^2}{M^2}} - \frac{\phi^\sigma(u_0)}{3u_0} e^{-\frac{-s_0^1 + m_{D_s}^2}{M^2}} \\
&\left. + \int_0^{u_0} d\alpha_1 \int_0^{1-u_0} \frac{d\alpha_2}{\alpha_3} \frac{16m_{f_0} f_{3f_0}^s \phi_{3f_0}^s(\alpha_i)}{[m_c^2 - q^2 + (\alpha_2 + v_0 \alpha_3)^2 m_{f_0}^2]} e^{-\frac{-s_0^1 + m_{D_s}^2}{M^2}} \right\}, \quad (61)
\end{aligned}$$

$$f_T^{S3}(q^2) = \frac{(m_c + m_s)(m_{D_s} + m_{f_0}) m_c m_{f_0}}{m_{D_s}^2 f_{D_s}} \left\{ \int_{u_0}^1 \frac{du}{u} \frac{\phi^\sigma(u)}{3M^2} e^{-\frac{-s_2(u) + m_{D_s}^2}{M^2}} + \frac{\phi^\sigma(u_0)}{3[m_c^2 - q^2 + u_0^2 m_{f_0}^2]} e^{-\frac{-s_0^1 + m_{D_s}^2}{M^2}} \right\}. \quad (62)$$

FFs	LCSRs-S ₁	LCSRs-S ₂	LCSRs-S ₃	3pSRs[3]	3pSRs[7]	LFQM[6]	CLFD/DR[1]	LCSRs[30]
$f_+(0)$	0.58 ± 0.07	0.40 ± 0.06	$0.78^{+0.13}_{-0.10}$	0.80 ± 0.08	0.96	0.87	0.86/0.90	0.30 ± 0.03
$f_-(0)$	$-0.10^{+0.04}_{-0.03}$	-0.40 ∓ 0.06	0.21 ± 0.04	—	—	—	0	—
$f_T(0)$	0.79 ± 0.13	0.95 ± 0.16	$0.47^{+0.07}_{-0.06}$	—	—	—	—	—

TABLE VI. $D_s \rightarrow f_0$ form factors at the full recoiled point obtained from various theoretical work under the $\bar{s}s$ description of f_0 .

The threshold momentum fraction is the solution of $s_i(u_0) = s_0$ with $i = 1, 2$,

$$u_0^i = \frac{-(s_0^i - q^2 - m_{f_0}^2) + \sqrt{(s_0^i - q^2 - m_{f_0}^2)^2 + 4m_{f_0}^2(m_c^2 - q^2)}}{2m_{f_0}^2}. \quad (63)$$

The expressions in Eqs. (55-56), Eqs. (58-59) and Eqs. (60-62), under different scenarios of the currents, are consistent with the result obtained in Ref. [30], Ref. [31] and Ref. [25], respectively. The above calculations are based on the ideal two-quark configuration that f_0 is pure an $s\bar{s}$ state. Nevertheless, there are several experiment measurements indicate the mixing between f_0 and σ ,

$$\sigma = |\bar{n}n\rangle \cos \theta + |\bar{s}s\rangle \sin \theta, \quad f_0 = -|\bar{n}n\rangle \sin \theta + |\bar{s}s\rangle \cos \theta. \quad (64)$$

Then the form factor in Eqs. (55-56), Eqs. (58-59) and Eqs. (60-62) are modified³ by multiplying an angle dependence $\cos \theta$. The mixing angle extracted from the data is not larger than 40° [32–34], and a recent LHCb measurement of the upper limit on the branching fraction $\mathcal{B}(\bar{B}^0 \rightarrow J/\Psi f_0) \times \mathcal{B}(f_0 \rightarrow \pi^+ \pi^-)$ leads to $|\theta| < 30^\circ$ [35]. In the follow calculation, we would take the mixing angle $\theta = 20^\circ \pm 10^\circ$.

The value of Borel mass squared is implied by the internal virtuality of propagator which is smaller than the cutoff threshold value, saying $M^2 \sim \mathcal{O}(um_{D_s}^2 + \bar{u}q^2 - u\bar{u}m_{f_0}^2) < s_0$, this value is a litter bit larger than the factorisation scale we chosen at $\mu_f^2 = m_{D_s}^2 - m_c^2 = 1.48^2 \text{ GeV}^2$ with the quark mass $\bar{m}_c(m_c) = 1.30 \text{ GeV}$. In practice the selection of Borel mass is actually a compromise between the overwhelming chosen of ground state in hadron spectral that demands a small value and the convergence of OPE evaluation that prefers a large one, which result in a region where $H_{ij}(q^2)$ shows an extremum in M^2

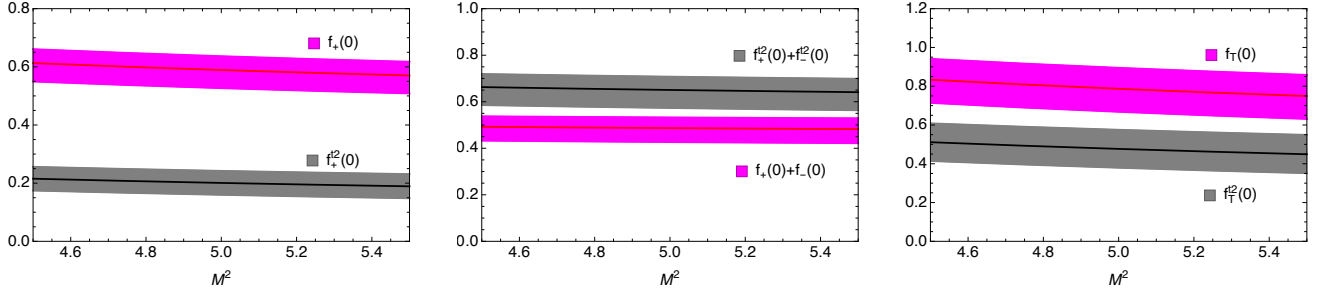
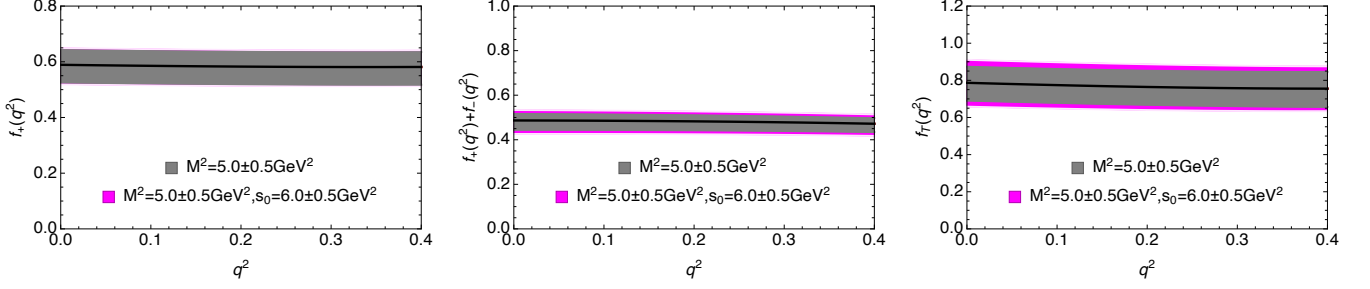
$$\frac{d}{d(1/M^2)} \ln H_{ij}(q^2) = 0. \quad (65)$$

The continuum threshold is usually set to close to the outset of the first excited state with the same quantum number as D_s and characterised by $s_0 \approx (m_{D_s} + \chi)^2$, which is finally determined by considering the maximal stable evolution of physical quantities on the Borel mass squared. We take $s_0 \equiv s_0^1 = s_0^2$ in the numerics. The chose of these two parameters should guaratee the convergence of twist expansion in the truncated OPE calculation (high twists contributions are no more than thirty percents) and simultaneously the high energy cutoff in the hadron interpolating (the contributions from high excited state and continuum spectral is smaller than thirty percents). We finally set them at $M^2 = 5.0 \pm 0.5 \text{ GeV}^2$ and $s_0 = 6.0 \pm 0.5 \text{ GeV}^2$ in this work. The value of Borel mass is a litter bit larger than it chosen in the $D_s \rightarrow \pi, K$ transition[36], close to it chosen in the $D_s \rightarrow \phi$ [30], $D_s \rightarrow \eta'$ [2] and $D_s \rightarrow f_0(980)$ transition [3].

We show the LCSRs result of $D_s \rightarrow f_0(980)$ form factors in table VI, the results obtained from other approaches are also presented parallel for comparison. We see that the result obtained by adopting different currents (S₁, S₂, S₃) are different, especially for the form factors f_+ which gives the contribution to semileptonic $D_s^+ \rightarrow f_0 e^+ \nu$ decays. The difference can be traced back to the ill-defined sum rules with the chiral currents under scenario S₂ and S₃, in which only the axial-vector current $\bar{s}\gamma_\mu\gamma_5 c$ is considered in the $D_s \rightarrow f_0$ decay while the vector current $\bar{s}\gamma_\mu c$ with the $D_{s_0}^* \rightarrow f_0$ decay is overlooked at the hadron level. Hereafter we would pay attention on the sum rules with the current chosen under scenario S₁. Our result $f_+(0) = 0.58 \pm 0.07$ is much larger than the previous LCSRs calculation $f_+(0) = 0.30 \pm 0.03$ [30], but more consistent with the recent measurement 0.52 ± 0.05 at BESIII [18]. The main reason of the difference is the input of decay constant \tilde{f}_{f_0} , which is taken at 180 MeV [5] in the previous work but 335 MeV evaluated from QCDSR here. Besides it, we have added the first gegenbauer expansion terms in the LCDAs which part contributions are ignored in the previous work.

We show the dependence of form factors on the Borel mass in figure 5, where the gray and magnate curves correspond to the result obtained up to leading twist and subleading twist LCDAs, the uncertainties come from the threshold value s_0 . We see that the subleading twist contribution is dominate in the form factors f_+ , while the leading twist contribution become more important for the form factor f_- and f_T . We plot the q^2 dependence of the form factors in figure 6 with the LCSRs maximal

³ The mixing would not bring changes to the LCSRs in section II since the angle dependence could be absorbed in to the definition of scalar decay constant.

FIG. 5. The Borel mass dependence of $D_s \rightarrow f_0$ form factors from the LCSRs.FIG. 6. The q^2 dependence of $D_s \rightarrow f_0$ form factors from the LCSRs.

momentum transfer $q_{\max}^2 = 0.4 \text{ GeV}^2$ [37], where the uncertainties associated to the Borel mass M^2 and also the threshold value s_0 are shown in the gray and magenta bands, respectively. We find that the uncertainties of LCSR's prediction to $D_s \rightarrow f_0$ form factors is full dominated by M^2 . To estimate the uncertainties associated to scale μ_f , we vary the charm quark mass in the region $\bar{m}_c(m_c) = 1.30 \pm 0.30 \text{ GeV}$ which result in $\mu_f = 1.48 \pm 0.30 \text{ GeV}$, we find this variation bring another 20% uncertainty to $f_+(q^2)$ and $f_T(q^2)$, and bring much significant corrections to $f_-(q^2)$ (large than 50%).

A. $B_s \rightarrow f_0$ form factors

With the definitions of heavy to light transition form factors in Eq. (44), we can straightly obtain the $B_s \rightarrow f_0$ form factor by substituting the charm quark to bottom quark in the LCSR's result shown in Eqs. (55-56). We take the bottom quark mass at $\bar{m}_b(m_b) = 4.2 \text{ GeV}$ and the factorization scale at $\mu_f = \mathcal{O}(m_{B_s}^2 - m_b) = 3 \text{ GeV}$ following the work in Ref. [38]. The Borel mass and threshold value are chosen at $M^2 = 18 \pm 2 \text{ GeV}^2$ and $s_0 = 36 \pm 2 \text{ GeV}^2$ closing to the choice in the previous LCSR's work [30]. In table VII, we present the $B_s \rightarrow f_0$ form factors at the full recoiled point obtained from various theoretical approaches, like the perturbative QCD(PQCD) [39], QCDSR [40], LCSR's with chiral current [31], LCSR's with light meson on-shell [30], LCSR's with B meson on-shell [24]. Again, our result with different weak vertex currents (S_1, S_2, S_3) have large difference and we focus on the result obtained under scenario S_1 with the axial-vector weak current. Our result is very close to the previous LCSR's result with the chiral current [31] which we would like to consider it as an incident. With using the same LCDAs of f_0 , our result is different from the result obtained in previous LCSR's [30], this is largely because of the different input of scalar coupling \hat{f}_{f_0} too. We can see also that our result of $f_+(0)$ is very close to it obtained in the LCSR's with the B meson LCDAs [24], while the form factors $f_-(0)$ and $f_T(0)$ have large deviations, so the high order corrections are highly eager to improve the accuracy. Here we estimate the possible NLO correction by varying the factorization scale as $\mu_f = 3.0 \pm 0.5 \text{ GeV}$, which in turn brings another 20% – 30% uncertainty to $f_+(q^2)$, $f_-(q^2)$ and $f_T(q^2)$.

In figure 7 we depict the Borel mass dependence of $B_s \rightarrow f_0$ form factors where the LCSR's result with the accuracy up to leading twist and subleading twist LCDAs are shown in gray and magenta curves, respectively. Due to the much better

FFs	LCSR _s - S_1	LCSR _s - S_2	LCSR _s - S_3	PQCD[39]	QCDSR[40]	LCSR-chiral[31]	LCSR _s [30]	LCSR _s [24]
$f_+(0)$	$0.45^{+0.09}_{-0.07}$	0.71 ± 0.17	0.19 ± 0.02	0.70	0.12	0.44	0.37	0.52
$f_-(0)$	$-0.41^{+0.11}_{-0.12}$	-0.71 ∓ 0.17	-0.13 ∓ 0.03	0	—	-0.44	0	0.04
$f_T(0)$	$0.54^{+0.09}_{-0.12}$	$0.89^{+0.20}_{-0.22}$	0.16 ± 0.02	0.40	-0.08	0.58	0.228	0.21

TABLE VII. $B_s \rightarrow f_0$ form factors at the full recoiled point obtained from various theoretical work under the $\bar{s}s$ description of f_0 .

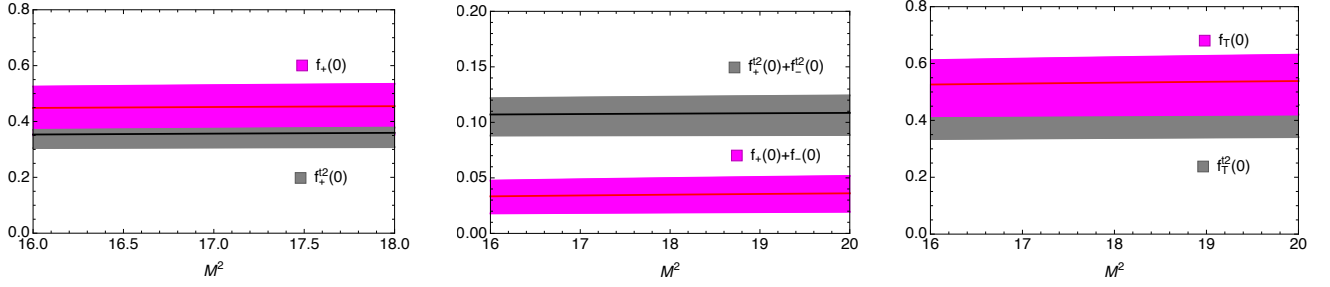


FIG. 7. The Borel mass dependence of $B_s \rightarrow f_0$ form factors from the LCSR.

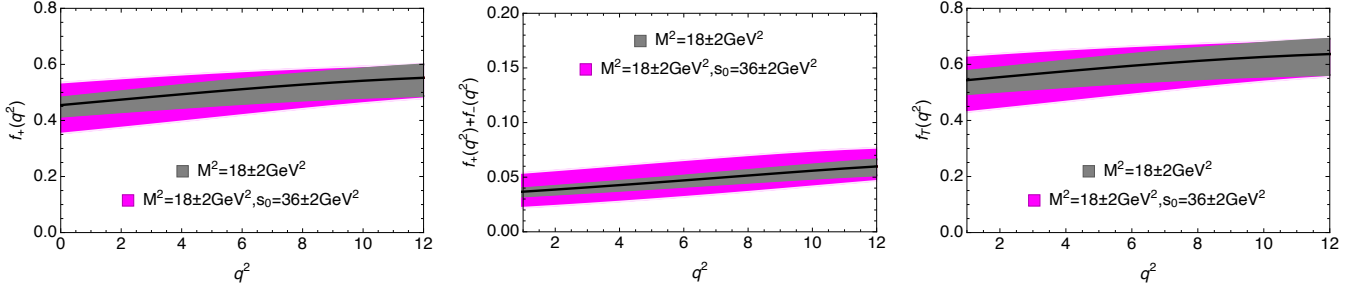


FIG. 8. The q^2 dependence of $B_s \rightarrow f_0$ form factors from the LCSR.

heavy quark expansion convergence in contrast to the D_s decay, we see that the leading twist contribution is the dominate one in $B_s \rightarrow f_0$ transition. We plot the momentum transfer dependence in figure 8 with the largest momentum transfer at $q_{\max}^2 = 12 \text{ GeV}^2$, where the uncertainties associated to Bore mass and also threshold value are overlap drawing in gray and magenta curves. We see that the dominate source of uncertainty comes from both the them.

B. $D_s^+ \rightarrow (f_0 \rightarrow) [\pi\pi]_S e^+ \nu_e$ decay

The second-order differential decay width of semileptonic decays $D_s^+(p) \rightarrow f_0(p_1)e^+(p_2)\nu_e(p_3)$ is proportional to the transition form factor f_1 as

$$\frac{d^2\Gamma(D_s^+ \rightarrow f_0 e^+ \nu_e)}{dE_2 dq^2} = \frac{G_F^2 m_{D_s}^2 |V_{cs}|^2}{16\pi^3} |f_1(q^2)|^2 [2x(1+y-z) - 4x^2 - y], \quad (66)$$

in which the dimensionless quantities are

$$x \equiv \frac{E_2}{m_{D_s}} \quad y \equiv \frac{q^2}{m_{D_s}^2}, \quad z \equiv \frac{m_{f_0}^2}{m_{D_s}^2} \quad (67)$$

with E_2 being the energy of lepton and $q^2 \equiv m_{23}^2 = (p_2 + p_3)^2 = (p - p_1)^2$ being the invariant mass of lepton-neutrino pair. Integrating over the lepton energy, we obtain the differential decay width on the momentum transfers q^2

$$\frac{d\Gamma(D_s^+ \rightarrow f_0 e^+ \nu_e)}{dq^2} = \frac{G_F^2 |V_{cs}|^2 \lambda^{3/2}(m_{D_s}^2, m_{f_0}^2, q^2)}{192\pi^3 m_{D_s}^3} |f_+(q^2)|^2. \quad (68)$$

$\lambda(a, b, c) = a^2 + b^2 + c^2 - 2xy - 2xz - 2yz$ is the Källén function.

From the experimental side, f_0 is measured via the $[\pi\pi]_S$ invariant mass spectral. So the key question in the phenomena is to look close at the role of f_0 in the $\pi\pi$ invariant mass. A natural solution is to examine the effects of resonance width, and noticeability, $D_s(p) \rightarrow [\pi(k_1)\pi(k_2)]_S l(p_2)\nu(p_3)$ decay is the kinematically simplest channel, because the invariant amplitude depends only on the invariant mass of dipion system $s \equiv p_1^2 = (k_1 + k_2)^2$ and not rely on its angular orientation with respecting the the remaining particles, meanwhile it is the most important channel due to the $[\pi\pi]_S$ phase shift shows a very board rise.

To perform with the BESIII analysis [18], we take the Flatté model to describe the width effect of intermediate resonant. The second-order differential decay width of $D_s^+ \rightarrow (f_0 \rightarrow) [\pi\pi]_S e^+ \nu_e$ is then written in

$$\frac{d^2\Gamma(D_s^+ \rightarrow [\pi\pi]_S e^+ \nu_e)}{dE_2 dq^2} = \frac{1}{\pi} \int_{4m_\pi^2}^{s_{\max}} ds \frac{g_1^2 \beta_{\pi\pi}}{|s - m_S^2 + i(g_1^2 \beta_{\pi\pi} + g_2^2 \beta_{KK})|^2} \frac{d^2\Gamma(D_s^+ \rightarrow Sl^+ \nu)}{dE_2 dq^2}. \quad (69)$$

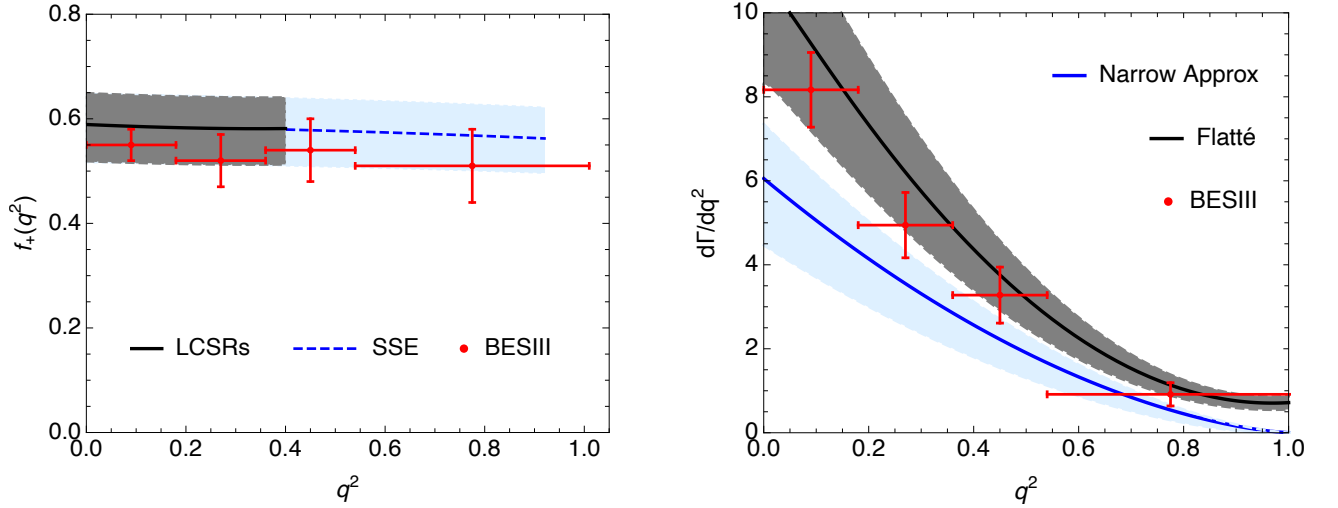


FIG. 9. Left: The LCSR prediction (gray) and the SSE parameterization (lightblue) of $D_s \rightarrow f_0$ form factor $f_+(q^2)$. Right: The differential width (in unit of $\text{ns}^{-1}/\text{GeV}^2/c^4$) of $D_s^+ \rightarrow f_0 e^+ \nu_e$ obtained from the narrow width approximation (blue) and the Flatté resonant formula (black).

$\beta_{\pi\pi}(s) = \sqrt{1 - 4m_\pi^2/s}$ and $\beta_{KK}(s) = \sqrt{1 - 4m_K^2/s}$ are the dipion phase factors, $g_1^2 = 0.165 \text{ GeV}^2$ and $g_2^2 = 0.695 \text{ GeV}^2$ are the weighted parameters [41]. Integrating over the invariant mass one arrives at the differential decay width on the momentum transfers

$$\frac{d\Gamma(D_s^+ \rightarrow [\pi\pi]_S e^+ \nu_e)}{dq^2} = \frac{1}{\pi} \frac{G_F^2 |V_{cs}|^2}{192\pi^3 m_{D_s}^3} |f_+(q^2)|^2 \int_{4m_\pi^2}^{s_{\max}} ds \frac{\lambda^{3/2}(m_{D_s}^2, s, q^2) g_1^2 \beta_{\pi\pi}(s)}{|s - m_S^2 + i(g_1^2 \beta_{\pi\pi}(s) + g_2^2 \beta_{KK}(s))|^2}. \quad (70)$$

In the left panel of figure 9, we depict the $D_s \rightarrow f_0$ form factor $f_+(q^2)$ obtained by the LCSR calculation in the large recoiled regions (gray band) and the simple z -series expansion parameterization (SSE) [42] in the small recoiled region (lightblue band). For the sake of comparison, we also plot the extracted form factor from the differential width $d\Gamma/dq^2$ measured at BESIII with the Flatté model. Our prediction is consistent with the data extraction, while shows a litter bit larger. In the right panel, we depict the differential width of $D_s^+ \rightarrow [\pi\pi]_S e^+ \nu_e$ on the momentum transfers, where the result obtained from the narrow width approximation in Eq. (68) and the Flatté resonant model in Eq. (70) are plotted in blue and black curves, respectively. The curve of decay width obtained from the narrow width approximation is a litter bit lower than the data, the result with considering the width effect by resonant model is in consistent with the data with showing a litter bit larger. This difference indicates the sensitive of differential decay width on the resonant model. Based on the discussions, we would like to comment that the extraction of $D_s \rightarrow f_0$ form factor by the BESIII measurement of differential decay width, as well as our result of decay width from the LCSR form factor, is model dependent. A model independent analysis is highly anticipated to do the high accuracy phenomena study.

IV. $D_s \rightarrow [\pi\pi]_S$ FROM FACTORS

A model independent study is to consider directly the stable $\pi\pi$ state on-shell rather than the f_0 . In this case the $D_s(p) \rightarrow [\pi(k_1)\pi(k_2)]_S l(p_2)\nu(p_3)$ decay amplitude can be written as

$$\mathcal{M}(D_s^+ \rightarrow [\pi\pi]_S e^+ \nu) = -\frac{iG_F}{\sqrt{2}} V_{cs}^* \bar{u}_e(p_2) \gamma^\mu (1 - \gamma_5) v_{\nu_4}(p_3) \langle [\pi(k_1)\pi(k_2)]_S | \bar{s} \gamma_\mu (1 - \gamma_5) c | D_s^+(p) \rangle, \quad (71)$$

in which the hadron transition matrix element is decomposed in terms of the orthogonal form factors

$$\langle [\pi(k_1)\pi(k_2)]_S | \bar{s} \gamma_\mu (1 - \gamma_5) c | D_s^+(p) \rangle = -iF_t(q^2, s, \zeta) k_\mu^t - iF_0(q^2, s, \zeta) k_\mu^0 - iF_\parallel(q^2, s, \zeta) k_\mu^\parallel \quad (72)$$

accompanying with the kinematical variables

$$k_\mu^t = \frac{q_\mu}{\sqrt{q^2}}, \quad k_\mu^0 = \frac{2\sqrt{q^2}}{\sqrt{\lambda_{D_s}}} \left(k_\mu - \frac{k \cdot q}{q^2} q_\mu \right), \quad k_\mu^\parallel = \frac{1}{\sqrt{k^2}} \left(\bar{k}_\mu - \frac{4(q \cdot k)(q \cdot \bar{k})}{\lambda_{D_s}} k_\mu + \frac{4k^2(q \cdot \bar{k})}{\lambda_{D_s}} q_\mu \right). \quad (73)$$

Besides the momentum transfers q^2 in the weak decay and the invariant mass $k^2 \equiv (k_1 + k_2)^2$ of dipion system, $D_s \rightarrow [\pi\pi]_S$ form factors also carries the information about the angular momentum between two collinear pions by the variable $2q \cdot \bar{k} \equiv 2q \cdot (k_1 - k_2) = \sqrt{\lambda_{D_s}}(2\zeta - 1) = \sqrt{\lambda_{D_s}}\beta_{\pi\pi}(k^2) \cos\theta_\pi$. Here θ_π is the angle between the 3-momenta of $\pi(k_2)$ meson and the $D_s(p)$ meson in the dipion rest frame, the Källén function is $\lambda_{D_s} = \lambda(m_{D_s}^2, k^2, q^2)$.

Multiplying Eq. (72) by the polarization vector of weak (lepton-neutrino pair) current, we can define the helicity form factors

$$H_i^{D_s \rightarrow [\pi\pi]_S}(q^2, k^2, \zeta) = \bar{e}^\mu(i) \langle [\pi(k_1)\pi(k_2)]_S | \bar{s}\gamma_\mu(1 - \gamma_5)c | D_s^+(p) \rangle. \quad (74)$$

The subscript $i = 0, t$ denotes the polarization direction, hereafter we would not show explicitly the superscript for the sake of simplicity. We immediately obtain the simple relation between the helicity form factors and the orthogonal form factors,

$$H_0(q^2, k^2, \zeta) = -iF_0(q^2, k^2, \zeta), \quad H_t(q^2, k^2, \zeta) = -iF_t(q^2, k^2, \zeta). \quad (75)$$

We then obtain the three-order differential width of semileptonic decay $D_s^+(p) \rightarrow [\pi(k_1)\pi(k_2)]_S e^+(p_2)\nu_e(p_3)$

$$\frac{d^3\Gamma(D_s^+ \rightarrow [\pi\pi]_S l^+\nu)}{dk^2 dq^2 d(\cos\theta_\pi)} = \frac{G_F^2 |V_{cs}|^2 \beta_{\pi\pi}(k^2) \sqrt{\lambda_{D_s}} q^2}{192\pi^3 m_{D_s}^3 16\pi} [-iF_0(q^2, k^2, \zeta)]^2. \quad (76)$$

The key issue becomes to calculate the $D_s \rightarrow [\pi\pi]_S$ form factors $F_0(q^2, k^2, \zeta)$.

A. The chiral even generalized 2π distribution amplitudes

In order to calculate the $D_s \rightarrow [\pi\pi]_S$ form factors, we should firstly know the LCDAs (2π DAs) of $\pi\pi$ system. We introduce a parameter angle to describe the mixing between $\bar{n}n = (\bar{u}u + \bar{d}d)/\sqrt{2}$ and $\bar{s}s$ in the isoscalar scalar $\pi\pi$ and KK states

$$[\pi\pi]_S = |\bar{n}n\rangle \cos\theta + |\bar{s}s\rangle \sin\theta, \quad [KK]_S = -|\bar{n}n\rangle \sin\theta + |\bar{s}s\rangle \cos\theta. \quad (77)$$

The chiral even two quark isoscalar 2π DAs [43, 44] involved in our calculation is defined by

$$\langle [\pi^a(k_1)\pi^b(k_2)]_S | \bar{s}(xn)\gamma_\mu s(0) | 0 \rangle = 2\delta^{ab} k_\mu \sin\theta \int du e^{iux(k \cdot n)} \Phi_{\parallel, [\pi\pi]_S}^{I=0}(u, \zeta, k^2). \quad (78)$$

It is easy to check the C -parity symmetry properties

$$\Phi_{\parallel, [\pi\pi]_S}^{I=0}(u, \zeta, k^2) = -\Phi_{\parallel, [\pi\pi]_S}^{I=0}(1-u, \zeta, k^2) = \Phi_{\parallel, [\pi\pi]_S}^{I=0}(u, 1-\zeta, k^2). \quad (79)$$

To describe the $\pi\pi$ system, three independent kinematical variables are introduced, they are the momentum fraction u carried by the antiquark with respect to the total momentum k , the longitudinal momentum fraction $\zeta = k_1^+/k^+$ carried by one pion in the system, and the invariant mass square $k^2 = s$.

The generalized isoscalar scalar 2π DAs is normalized by the quark part of energy momentum tensor form factor F_π^{EMT} ,

$$\int du (2u-1) \Phi_{\parallel, [\pi\pi]_S}^{I=0}(u, \zeta, k^2) = -2M_2^{(\pi)} \zeta (1-\zeta) F_\pi^{\text{EMT}}(k^2), \quad (80)$$

in which $M_2^{(\pi)}$ indicates the second moment of quark distributions in the pion $M_2^{(\pi)} = 2 \int_0^1 du u [q_\pi(u) + \bar{q}_\pi(x)]$, $F_\pi^{\text{EMT}}(0) = 1$.

With the double expansion of eigenfunction of the evolution function and the partial wave, the generalized 2π DAs is written by the detached Gegenbauer and Legendre polynomials

$$\Phi_{\parallel, [\pi\pi]_S}^I(u, \zeta, k^2, \mu) = 6u(1-u) \sum_{n=1, \text{odd}}^{\infty} \sum_{l=0, \text{even}}^{n+1} B_{\parallel, nl}^{I=0}(k^2, \mu) C_n^{3/2}(2u-1) C_l^{1/2}(2\zeta-1). \quad (81)$$

The k^2 -dependent expansion coefficient B_{nl} have the similar scale evolution as the gegenbauer coefficients in the LCDAs of f_0 meson [45].

$$B_{\parallel, nl}^{I=0}(\mu, k^2) = B_{\parallel, nl}^{I=0}(0) \left[\frac{\alpha_s(\mu)}{\alpha_s(\mu_0)} \right]^{\frac{\gamma_n^{(0)} - \gamma_0^{(0)}}{(2\beta_0)}} \text{Exp} \left[\sum_{m=1}^{N-1} \frac{k^{2m}}{m!} \frac{d^m}{dk^{2m}} \ln B_{\parallel, nl}^{I=0}(0) + \frac{k^{2N}}{\pi} \int_{4m_K^2}^{\infty} ds \frac{\delta_l^{I=0}(s)}{s^N (s - k^2 - i0)} \right]. \quad (82)$$

the pion-pion phase shift $\delta_l^{I=0}(s)$ carries the resonant information in the dipion invariant mass spectral. At one-loop level, the anomalous dimension reads as

$$\gamma_n^{\parallel,(0)} = 8C_F \left(\sum_{k=1}^{n+1} \frac{1}{k} - \frac{3}{4} - \frac{1}{2(n+1)(n+2)} \right), \quad (83)$$

the β function coefficient is $\beta_0 = 11 - 2N_f/3$. Based on the Watson theorem of scattering amplitudes, the exponential function in Eq. (82) is the solution of the N -subtracted dispersion relation for the coefficient B_{nl} , whose evolution could touch up to ~ 2.5 GeV.

Concerning the coefficients at the zero point of invariant mass, the soft pion theorem and the crossing symmetry relate it with the gegenbauer moments a_n and the moments of quark distribution M_N in pion.

$$\sum_{l=0}^{n+1} B_{\parallel,nl}^{I=0} = 0, \quad B_{\parallel,N-1N}^{I=0}(0) = \frac{1}{3} \frac{2N+1}{N+1} M_{N=\text{even}}^{(\pi)}. \quad (84)$$

In the vicinity of the resonance, isoscalar scalar 2π DAs deduces to the distribution amplitudes of f_0

$$\bar{f}_{f_0} a_n^{f_0} = B_{\parallel,n0}^{I=0}(0) \text{Exp} \left[\sum_{m=1}^{n-1} c_m^{(n0)} m_{f_0}^{2m} \right], \quad \bar{f}_{f_0} a_1^{f_0} = \frac{\Gamma_{f_0} \text{Im} B_{\parallel,12}^{I=0}(m_{f_0}^2)}{g_{f_0\pi\pi}} \quad (85)$$

with the subtraction coefficient

$$c_m^{(nl)} = \frac{1}{m!} \frac{d^m}{dk^{2m}} \left[\ln B_{\parallel,nl}^{I=0}(k^2) - \ln B_{\parallel,l+1l}^{I=0}(k^2) \right]_{k^2 \rightarrow 0}. \quad (86)$$

Based on the QCDSR calculation of LCDAS of f_0 in the section II, we obtain the first expansion and subtraction coefficients of isoscalar scalar dipion system.

$$\begin{aligned} \bar{f}_{f_0} a_1^{f_0} &= B_{\parallel,10}^{I=0}(0) = \frac{\Gamma_{f_0} \text{Im} B_{\parallel,10}^{I=0}(m_{f_0}^2)}{g_{f_0\pi\pi}} = -0.300, \quad B_{\parallel,12}^{I=0} = -B_{\parallel,10}^{I=0} = 0.300, \\ \frac{d \ln B_{\parallel,10}^{I=0}(k^2)}{dk^2} \Big|_{k^2 \rightarrow 0} &= \frac{d \ln B_{\parallel,12}^{I=0}(k^2)}{dk^2} \Big|_{k^2 \rightarrow 0} = \frac{N_c}{48\pi^2 f_\pi^2} = 0.375. \end{aligned} \quad (87)$$

In figure 10, we depict the phase shift $\delta_l^{I=0}(s)$ from the amplitude analysis with a combination of dispersion relations and unitarity [46, 47], and the obtained expansion coefficient $B_{l1}^{I=0}(s)$. We can clearly see a sharp dip around the f_0 region in the S -wave contribution to phase shift and hence the first-order expansion coefficient, additionally, a quick rising around $f_0(1370)$ region in the D -wave contributions.

B. $D_s \rightarrow [\pi\pi]_S$ from factor $F_0^{(l)}(q^2, s)$ at leading twist

To evaluate the $D_s \rightarrow [\pi\pi]_S$ form factors, we consider the nonlocal correlation function

$$\Pi_\mu^{ab}(q, k_1, k_2) = i \int d^4x e^{iq \cdot x} \langle \pi^a(k_1) \pi^b(k_2) | T \{ j_{1,\mu}^{S1}(x), j_2^{S1}(0) \} | 0 \rangle, \quad (88)$$

and take the D_s interpolating current and weak decay currents as the same as in the scenario I (S1) in the calculation of $D_s \rightarrow f_0$ form factors. Since our knowledge of 2π DAs is still at leading twist level so far, we can only discuss the width effect of $D_s \rightarrow [\pi\pi]_S$ at leading twist. We furthermore consider an auxiliary correlation function

$$\Pi^{ab}(q, k_1, k_2) = i \int d^4x e^{iq \cdot x} \langle \pi^a(k_1) \pi^b(k_2) | T \{ j_5(x), j_2^{S1}(0) \} | 0 \rangle. \quad (89)$$

to evaluate the timelike helicity form factor F_t with the weak current $j_5 = -im_c \bar{s} \gamma_5 c$. The auxiliary correlation function can be obtained by multiplying Eq. (88) with q_μ .

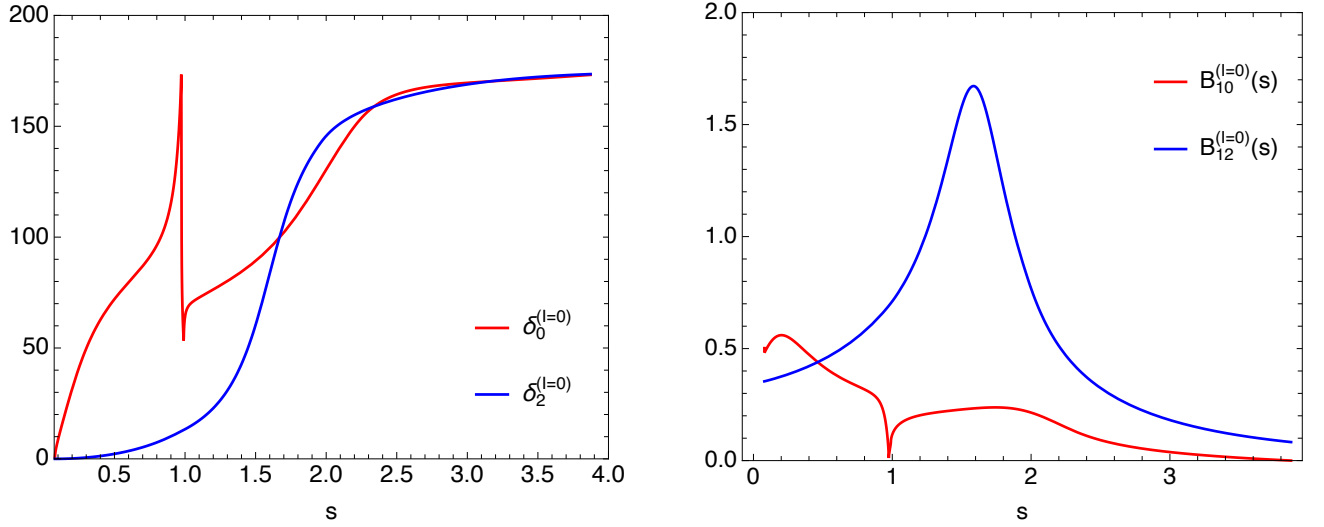


FIG. 10. The phase shifts $\delta_l^{(I=0)}(s)$ (left) and the expansion coefficients $B_{1l}^{(I=0)}(s)$ (right) of isoscalar $\pi\pi$ system in the S and D -waves.

For the sake of simplicity, we take the neutral dipion system with electric charge $a = b = 0$ for example to show the LCSR's evaluation. The correction functions in Eqs. (88,89) can be written in the hadron representation as

$$\begin{aligned} \Pi_\mu^{\text{had}}(q, k_1, k_2) &= \frac{im_{D_s}^2 f_{D_s}}{[m_{D_s}^2 - (k+q)^2] (m_c + m_s)} \left[F_t(q^2, k^2, \zeta) k_\mu^t + F_0(q^2, k^2, \zeta) k_\mu^0 + F_{\parallel}(q^2, k^2, \zeta) k_\mu^{\parallel} \right] \\ &+ \frac{1}{\pi} \int_{s_0}^{\infty} ds \frac{\rho_t^h(q^2, s) k_\mu^t + \rho_0^h(q^2, s) k_\mu^0 + \rho_{\parallel}^h(q^2, s) k_\mu^{\parallel}}{s - (k+q)^2}, \end{aligned} \quad (90)$$

$$\Pi^{\text{had}}(q, k_1, k_2) = \frac{m_{D_s}^2 f_{D_s}}{[m_{D_s}^2 - (k+q)^2] (m_c + m_s)} \left[\sqrt{q^2} F_t(q^2, k^2, \zeta) \right] + \frac{1}{\pi} \int_{s_0}^{\infty} ds \frac{\rho^h(q^2, s)}{s - (k+q)^2}. \quad (91)$$

Meanwhile, the OPE calculation of these correlation functions result in

$$\Pi_\mu^{\text{OPE}}(q, k_1, k_2) = 2i \sin \theta m_c k_\mu \int_0^1 \frac{du}{u} \frac{\Phi_{\parallel, [\pi\pi]_S}^{I=0, s\bar{s}}(u, \zeta, k^2)}{s'_2(u) - (k+q)^2}, \quad (92)$$

$$\Pi^{\text{OPE}}(q, k_1, k_2) = \frac{m_c \sin \theta}{2} \int_0^1 \frac{du}{u} \frac{\Phi_{\parallel, [\pi\pi]_S}^{I=0, s\bar{s}}(u, \zeta, k^2) [m_{D_s}^2 - q^2 - (1-2u)k^2]}{s'_2(u) - (k+q)^2}. \quad (93)$$

After applying the quark-hadron duality and Borel transformation, we obtain the relations between $D_s \rightarrow [\pi\pi]_S$ form factors

$$\frac{2\sqrt{q^2}}{\lambda_{D_s}} F_0(q^2, k^2, \zeta) - \frac{4(q \cdot k)(q \cdot \bar{k})}{\lambda_{D_s} \sqrt{k^2}} F_{\parallel}(q^2, k^2, \zeta) = \frac{2m_c(m_c + m_s) \sin \theta}{m_{D_s}^2 f_{D_s}} \int_{u_0}^1 \frac{du}{u} \Phi_{\parallel, [\pi\pi]_S}^{I=0, s\bar{s}}(u, \zeta, k^2) e^{-\frac{s'_2(u) - m_{D_s}^2}{M^2}}, \quad (94)$$

$$\frac{F_t(q^2, k^2, \zeta)}{\sqrt{q^2}} - \frac{2(q \cdot k) F_0(q^2, k^2, \zeta)}{\sqrt{\lambda_{D_s} q^2}} + \frac{4\sqrt{k^2}(q \cdot \bar{k}) F_{\parallel}(q^2, k^2, \zeta)}{\lambda_{D_s}} = 0. \quad (95)$$

Here $s'_2(u) = \bar{u}k^2 + (m_c^2 - \bar{u}q^2)/u$. The sum rules are ultimately obtained as

$$\cos \theta_\pi F_{\parallel}(q^2, k^2, \zeta) = \frac{m_c(m_c + m_s) \sin \theta}{m_{D_s}^2 f_{D_s} \sqrt{\lambda_{D_s} \beta_{\pi\pi}(k^2)}} \int_{u_0}^1 \frac{du}{u} \left[4u(k^2)^{3/2} \right] \Phi_{\parallel, [\pi\pi]_S}^{I=0, s\bar{s}}(u, \zeta, k^2) e^{-\frac{s'_2(u) - m_{D_s}^2}{M^2}}, \quad (96)$$

$$F_0(q^2, k^2, \zeta) = \frac{m_c(m_c + m_s) \sin \theta}{m_{D_s}^2 f_{D_s} \sqrt{\lambda_{D_s} \sqrt{q^2}}} \int_{u_0}^1 \frac{du}{u} \left[\lambda_{D_s} + 2uk^2(m_{D_s}^2 + q^2 - k^2) \right] \Phi_{\parallel, [\pi\pi]_S}^{I=0, s\bar{s}}(u, \zeta, k^2) e^{-\frac{s'_2(u) - m_{D_s}^2}{M^2}}, \quad (97)$$

$$\sqrt{q^2} F_t(q^2, k^2, \zeta) = \frac{m_c(m_c + m_s) \sin \theta}{m_{D_s}^2 f_{D_s}} \int_{u_0}^1 \frac{du}{u} \left[m_{D_s}^2 - q^2 - (1-2u)k^2 \right] \Phi_{\parallel, [\pi\pi]_S}^{I=0, s\bar{s}}(u, \zeta, k^2) e^{-\frac{s'_2(u) - m_{D_s}^2}{M^2}}. \quad (98)$$

We can check that $F_0(q^2, k^2, \zeta) = F_t(q^2, k^2, \zeta)$ at the full recoiled point $q^2 = 0$. From the view of partial-wave analysis [48], $D_s \rightarrow \pi\pi$ form factors are expanded by

$$F_{0,t}(q^2, k^2, \zeta) = \sum_{\ell=0}^{\infty} \sqrt{2\ell+1} F_{0,t}^{(\ell)}(q^2, k^2) P_{\ell}^{(0)}(\cos\theta_{\pi}),$$

$$F_{\parallel,\perp}(q^2, k^2, \zeta) = \sum_{\ell=0}^{\infty} \sum_{\ell'=0}^{\ell} \sqrt{2\ell'+1} F_{\parallel,\perp}^{(\ell')} (q^2, k^2) \frac{P_{\ell'}^{(1)}(\cos\theta_{\pi})}{\sin\theta_{\pi}}. \quad (99)$$

The associated Legendre polynomials have the orthogonality relations

$$\int_{-1}^1 P_{\ell}^n(x) P_k^n(x) dx = \frac{2}{2\ell+1} \frac{(\ell+n)!}{(\ell-n)!} \delta_{k\ell}, \quad \int_{-1}^1 \frac{P_{\ell}^m(x) P_{\ell'}^n(x)}{1-x^2} dx = \frac{(\ell+m)!}{m(\ell-m)!} \delta_{m'n} \quad \text{with } m, n \neq 0. \quad (100)$$

Multiplying $P_{\ell}^{(0)}(\cos\theta_{\pi})$ to both sides of Eqs. (96,97) and integrating over $\cos\theta_{\pi}$, we obtain the sum rules of $D_s \rightarrow [\pi\pi]_S$ form factors at ℓ' -wave ($\ell' = \text{even}$ and $\ell' \leq n+1$)

$$\sum_{\ell=1}^{\infty} I_{\ell'\ell}^{I=0} F_{\parallel}^{(\ell)}(q^2, k^2) = \frac{m_c(m_c + m_s) \sin\theta}{m_{D_s}^2 f_{D_s} \sqrt{\lambda_{D_s}}} \sum_{n=1, \text{odd}}^{\infty} \frac{1}{2\ell'+1} J_n^{\parallel}(q^2, k^2, M^2, s_0) B_{n\ell',\parallel}^{I=0}(k^2), \quad (101)$$

$$F_0^{(\ell')}(q^2, k^2) = \frac{m_c(m_c + m_s) \sin\theta}{m_{D_s}^2 f_{D_s} \sqrt{\lambda_{D_s}} \sqrt{q^2}} \sum_{n=1, \text{odd}}^{\infty} \frac{\beta_{\pi\pi}(k^2)}{\sqrt{2\ell'+1}} J_n^0(q^2, k^2, M^2, s_0) B_{n\ell',\parallel}^{I=0}(k^2), \quad (102)$$

$$F_t^{(\ell')}(q^2, k^2) = \frac{m_c(m_c + m_s) \sin\theta}{m_{D_s}^2 f_{D_s} \sqrt{q^2}} \sum_{n=1, \text{odd}}^{\infty} \frac{\beta_{\pi\pi}(k^2)}{\sqrt{2\ell'+1}} J_n^t(q^2, k^2, M^2, s_0) B_{n\ell',\parallel}^{I=0}(k^2), \quad (103)$$

with the conformal expansion functions J_n

$$J_n^{\parallel}(q^2, k^2, M^2, s_0) = 6 \int_{u_0}^1 du \bar{u} C_n^{3/2}(2u-1) \left[4(k^2)^{3/2} \right] e^{-\frac{s_2'(u) - m_{D_s}^2}{M^2}}, \quad (104)$$

$$J_n^0(q^2, k^2, M^2, s_0) = 6 \int_{u_0}^1 du \bar{u} C_n^{3/2}(2u-1) [\lambda_{D_s} + 2uk^2 (m_{D_s}^2 + q^2 - k^2)] e^{-\frac{s_2'(u) - m_{D_s}^2}{M^2}}, \quad (105)$$

$$J_n^t(q^2, k^2, M^2, s_0) = 6 \int_{u_0}^1 du \bar{u} C_n^{3/2}(2u-1) [m_{D_s}^2 - q^2 - (1-2u)k^2] e^{-\frac{s_2'(u) - m_{D_s}^2}{M^2}}. \quad (106)$$

and the additional partial-wave expansion function $I_{\ell'\ell}$

$$I_{\ell'\ell}^{I=0} = \sqrt{2\ell+1} \int_{-1}^1 d(\cos\theta_{\pi}) \frac{\cos\theta_{\pi}}{\sin\theta_{\pi}} P_{\ell''}^{(0)}(\cos\theta_{\pi}) P_{\ell}^{(1)}(\cos\theta_{\pi}). \quad (107)$$

We mark that $I_{\ell'\ell}^{I=0}$ is zero when ℓ goes over odd number, $I_{02}^{I=0} = -2\sqrt{5}$, $I_{22}^{I=0} = -4/\sqrt{5}$ and $I_{\ell'2}^{I=0} = 0$ when $\ell' > 2$.

In figure 11 we depict the evolutions of S -wave $D_s \rightarrow [\pi\pi]_S$ form factor on the momentum transfers (left panel) and invariant mass (right panel). and in figure 12 for the form factor with D -wave $\pi\pi$ system. We take the mixing angle between the isoscalar scalar $\pi\pi$ and KK systems at $\theta = 20^\circ \pm 10^\circ$ which is similar as the angle in the σ - f_0 mixing [32]. The uncertainty arose from the mixing angle is added up to the LCSRs parameters uncertainty and shown in the magenta bands. We find that the D -wave form factor $\sqrt{q^2} F_0^{(l=2)}(q^2)$ is much smaller than the S -wave $\sqrt{q^2} F_0^{(l=0)}(q^2)$ when the invariant mass is small, while in the resonant regions D -wave contribution is comparable or even larger than the S -wave.

C. $D_s \rightarrow [\pi\pi]_S e\nu_e$ decay at leading twist

In figure 13, we depict the evolution of form factor on the momentum transfers q^2 where the invariant mass dependence is integrated out.

$$\sqrt{q^2} F_0^{(l)}(q^2) = \int_{4m_{\pi}^2}^{s_{\max}(q^2)} ds \sqrt{q^2} F_0^{(l)}(q^2, s), \quad (108)$$

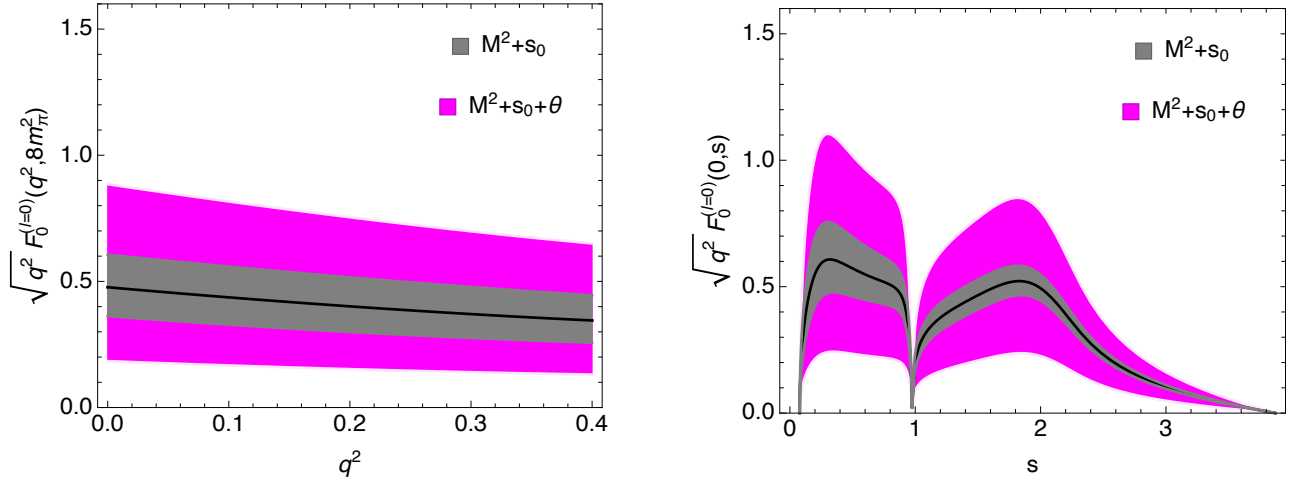


FIG. 11. Evolution of the S -wave orthogonal $D_s \rightarrow [\pi\pi]_S$ form factor on the momentum transfers $\sqrt{q^2} F_0^{(l=0)}(q^2, s = 8m_\pi^2)$ (left) and on the invariant mass $\sqrt{q^2} F_0^{(l=0)}(q^2 = 0, s)$ (right).

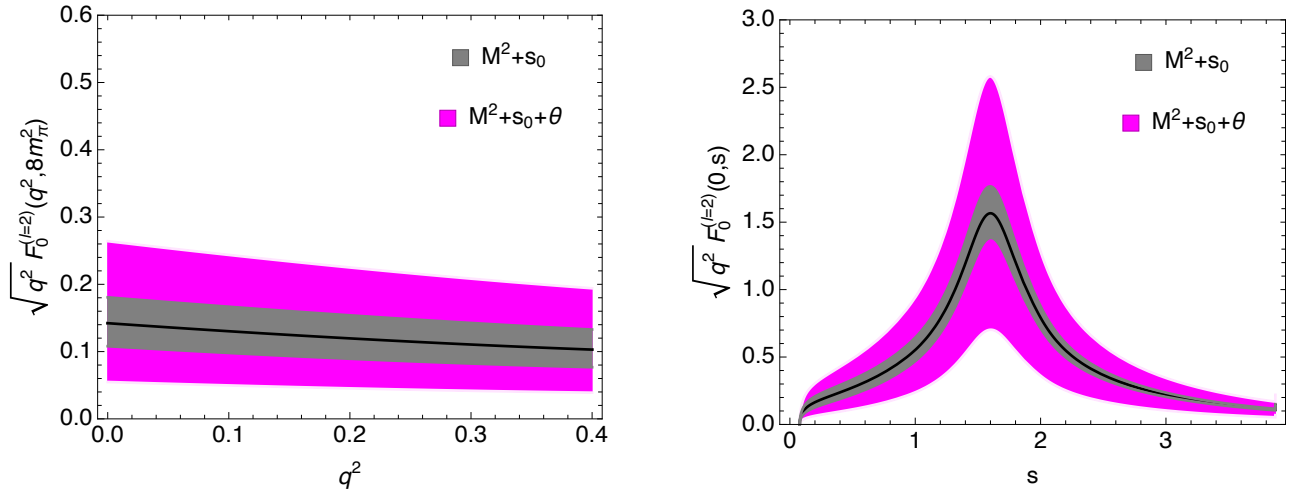


FIG. 12. The same as figure. 11, but for the D -wave $\pi\pi$ system.

here $s_{\max}(q^2)$ is the solution of $\lambda(m_{D_s}^2, q^2, s) = 0$. Again, the kinematical region with small recoling is extrapolated by the SSE parameterization.

Considering the partial-wave expansion of $D_s \rightarrow \pi\pi$ form factors in Eq. (99) and the orthogonal conditions in Eq. (100), the three-order differential decay width in Eq. (76) deduces to the second-order one after integrating over the angle θ_π ,

$$\frac{d^2\Gamma(D_s^+ \rightarrow [\pi\pi]_S l^+\nu)}{dk^2 dq^2} = \frac{G_F^2 |V_{cs}|^2}{192\pi^3 m_{D_s}^3} \frac{\beta_{\pi\pi}(k^2) \sqrt{\lambda_{D_s}}}{16\pi} \sum_{\ell=0}^{\infty} 2 |\sqrt{q^2} F_0^{(\ell)}(q^2, k^2)|^2. \quad (109)$$

After doing the integration on the invariant mass, we plot the momentum transfer dependence of the $D_s^+ \rightarrow [\pi\pi]_S e^+\nu_e$ decay width (in unit of $\text{ns}^{-1}/\text{GeV}^2/c^4$) in the right panel of figure. 14. We mark that the result is obtained at leading twist level of the the dipion LCDAs, so we compare it with the result obtained from the narrow width approximation and Flatté resonant model with the leading twist $D_s \rightarrow f_0$ form factor, which is shown in the left panel. The three curves of central value indicates from one side the sensitivity of predictions to the resonant model, and from another side that the direct calculation from $D_s \rightarrow [\pi\pi]$ form factor shows relatively moderate evolution with larger allowed momentum transfers. We mark again the subleading twist contribution is the dominate one in $D_s \rightarrow f_0$ form factors, so the further study on the twist three dipion LCDAs could provide a model independent solution to the four-body semileptonic decays of D_s meson.

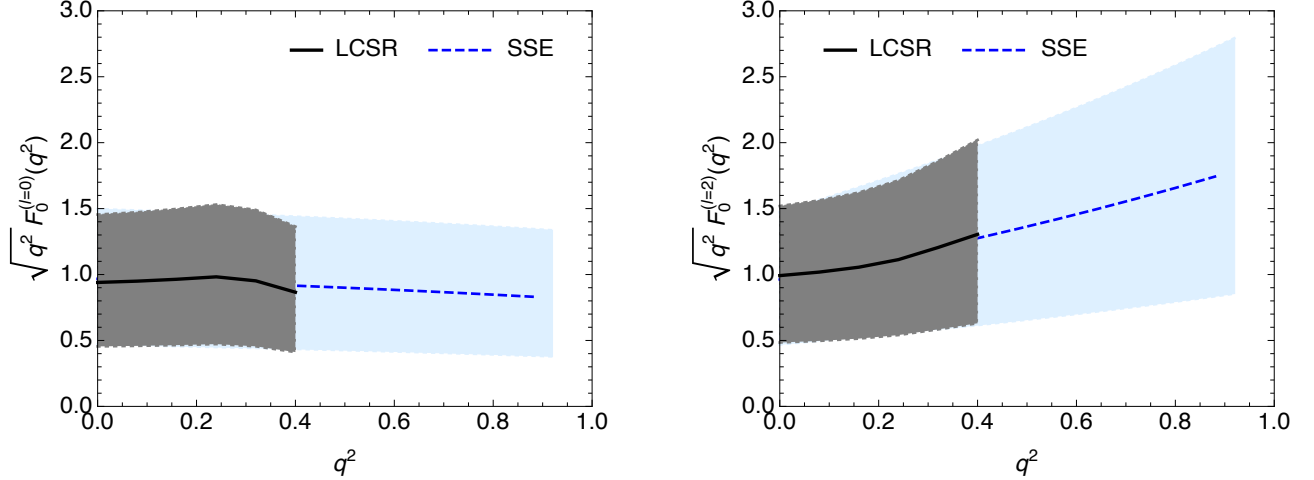


FIG. 13. The integrated form factor $\sqrt{q^2} F_0^{(l)}(q^2)$ for the S -wave (left) and D -wave (right) $\pi\pi$ system.

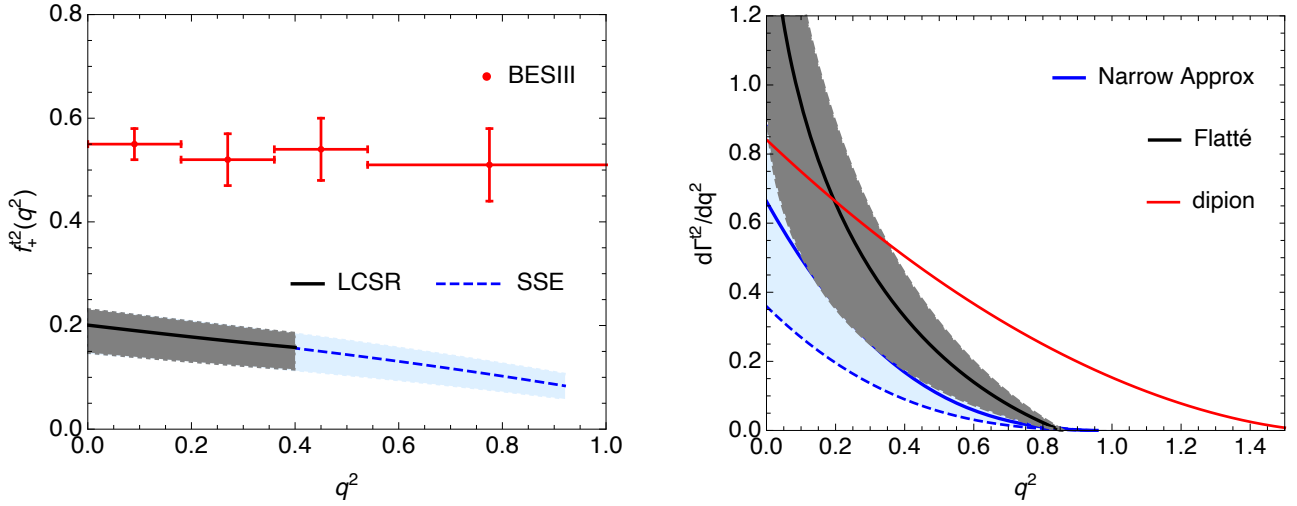


FIG. 14. The same as figure. 9, but for the leading twist contribution.

V. SUMMARY

In this work we firstly update the QCD sum rules predictions of isoscalar scalar meson f_0 , especially for the decay constant and the gegenbauer expansion coefficients in the LCDAs, followed which we calculate the $D_s \rightarrow f_0$ transition form factors from the LCSRs with f_0 LCDAs and obtain the differential width of semileptonic decay $D_s^+ \rightarrow f_0 e^+ \nu_e$. With the updated decay constant of f_0 which is about two times of the one used in the previous LCSRs calculation, our result of $D_s \rightarrow f_0$ form factors $f_+(q^2)$ with considering the mixing between $\bar{s}s$ and $\bar{u}u + \bar{d}d$ of f_0 is in consistent with the data extracted from the measurement of differential width in the whole momentum transfer region, indicating that the energetic picture of f_0 in charm meson decay is still reliable. The result of differential width obtained under the narrow width approximation shows a litter bit lower than the data, the result obtained under the intermediate resonant model with Flatté formula shows the consistence. In order to get rid of the model dependence and give more powerful prediction, we suggest to describe the unstable scalar meson by the dipion LCDAs and calculate the $D_s \rightarrow [\pi\pi]_S$ form factors. At leading twist, the directly calculation of differential width of $D_s^+ \rightarrow [\pi\pi]_S e^+ \nu_e$ decay exhibits a moderate evolution on the momentum transfers, comparing to the result obtained under the narrow width approximation and the Flatté model.

Our calculation of $D_s \rightarrow [\pi\pi]_S$ form factors is carried out at leading twist due to the finite knowledge of dipion LCDAs, so an important issue of further development in this project is to construct the twist three dipion LCDAs and take in to account their contributions. Of course, the next-to-leading-order QCD radiation corrections of the correlation function is also imperative to improve the prediction accuracy. This work reveals a bright prospect to study the four-body leptonic decays of heavy mesons with the dimeson light-cone distribution amplitudes, the future experiment with larger integrated luminosity [49, 50] would help

us to understand the LCDAs of dipion system much better.

VI. ACKNOWLEDGEMENTS

We are grateful to Ling-Yun Dai and Hai-Bo Li for fruitful discussions, especially to Hai-Yang Cheng for the careful reading of the draft and the helpful comments. SC is supported by the National Science Foundation of China (NSFC) under Grant No. 11975112. SLZ acknowledge the support from the Natural Science Foundation of Hunan Province, China under Contract No. 2021JJ40036 and the Fundamental Research Funds for the Central Universities under Contract No. 020400/531118010467.

-
- [1] B. El-Bennich, O. Leitner, J. P. Dedonder and B. Loiseau, *Phys. Rev. D* **79**, 076004 (2009)
 - [2] N. Offen, F. A. Porkert and A. Schäfer, *Phys. Rev. D* **88**, no.3, 034023 (2013)
 - [3] I. Bediaga and M. Nielsen, *Phys. Rev. D* **68**, 036001 (2003)
 - [4] H. Y. Cheng, C. K. Chua and K. C. Yang, *Phys. Rev. D* **73**, 014017 (2006)
 - [5] F. De Fazio and M. R. Pennington, *Phys. Lett. B* **521** (2001), 15-21
 - [6] H. W. Ke, X. Q. Li and Z. T. Wei, *Phys. Rev. D* **80**, 074030 (2009)
 - [7] T. M. Aliev and M. Savci, *EPL* **90**, no.6, 61001 (2010)
 - [8] M. Ablikim *et al.* [BESIII], *Phys. Rev. D* **103**, no.9, 092004 (2021)
 - [9] R. L. Jaffe, *Phys. Rev. D* **15** (1977), 267
 - [10] S. S. Agaev, K. Azizi and H. Sundu, *Phys. Lett. B* **781** (2018), 279-282
 - [11] J. D. Weinstein and N. Isgur, *Phys. Rev. Lett.* **48** (1982), 659
 - [12] J. D. Weinstein and N. Isgur, *Phys. Rev. D* **27** (1983), 588
 - [13] J. D. Weinstein and N. Isgur, *Phys. Rev. D* **41** (1990), 2236
 - [14] J. Yelton *et al.* [CLEO], *Phys. Rev. D* **80**, 052007 (2009)
 - [15] K. M. Ecklund *et al.* [CLEO], *Phys. Rev. D* **80**, 052009 (2009)
 - [16] J. Hietala, D. Cronin-Hennessy, T. Pedlar and I. Shipsey, *Phys. Rev. D* **92**, no.1, 012009 (2015)
 - [17] M. Ablikim *et al.* [BESIII], *Phys. Rev. D* **105**, no.3, L031101 (2022)
 - [18] M. Ablikim *et al.* [BESIII], [arXiv:2303.12927 [hep-ex]]
 - [19] J. Govaerts, L. J. Reinders, F. de Viron and J. Weyers, *Nucl. Phys. B* **283**, 706-722 (1987)
 - [20] K. C. Yang, W. Y. P. Hwang, E. M. Henley and L. S. Kisslinger, *Phys. Rev. D* **47**, 3001-3012 (1993)
 - [21] C. D. Lu, Y. M. Wang and H. Zou, *Phys. Rev. D* **75**, 056001 (2007)
 - [22] B. L. Ioffe, *Phys. Atom. Nucl.* **66**, 30-43 (2003)
 - [23] Z. H. Wu, H. B. Fu, T. Zhong, D. Huang, D. D. Hu and X. G. Wu, [arXiv:2211.05390 [hep-ph]]
 - [24] S. Cheng and J. M. Shen, *Eur. Phys. J. C* **80**, no.6, 554 (2020)
 - [25] H. Y. Han, X. G. Wu, H. B. Fu, Q. L. Zhang and T. Zhong, *Eur. Phys. J. A* **49**, 78 (2013)
 - [26] Y. M. Wang, M. J. Aslam and C. D. Lu, *Phys. Rev. D* **78** (2008), 014006
 - [27] V. M. Braun, G. P. Korchemsky and D. Müller, *Prog. Part. Nucl. Phys.* **51**, 311-398 (2003)
 - [28] J. Bijnens and A. Khodjamirian, *Eur. Phys. J. C* **26**, 67-79 (2002)
 - [29] P. Ball, V. M. Braun and A. Lenz, *JHEP* **05**, 004 (2006)
 - [30] P. Colangelo, F. De Fazio and W. Wang, *Phys. Rev. D* **81**, 074001 (2010)
 - [31] Y. J. Sun, Z. H. Li and T. Huang, *Phys. Rev. D* **83**, 025024 (2011)
 - [32] A. Gokalp, Y. Sarac and O. Yilmaz, *Phys. Lett. B* **609**, 291-297 (2005)
 - [33] R. Fleischer, R. Knegjens and G. Ricciardi, *Eur. Phys. J. C* **71** (2011), 1832
 - [34] H. Y. Cheng, C. W. Chiang and Z. Q. Zhang, *Phys. Rev. D* **105** (2022) no.3, 033006
 - [35] R. Aaij *et al.* [LHCb], *Phys. Rev. D* **87** (2013) no.5, 052001
 - [36] A. Khodjamirian, R. Ruckl, S. Weinzierl, C. W. Winhart and O. I. Yakovlev, *Phys. Rev. D* **62**, 114002 (2000)
 - [37] S. Cheng, Y. h. Ju, Q. Qin and F. s. Yu, *Eur. Phys. J. C* **82**, no.11, 1037 (2022)
 - [38] G. Duplancic, A. Khodjamirian, T. Mannel, B. Melic and N. Offen, *JHEP* **04** (2008), 014
 - [39] R. H. Li, C. D. Lu, W. Wang and X. X. Wang, *Phys. Rev. D* **79**, 014013 (2009)
 - [40] N. Ghahramany and R. Khosravi, *Phys. Rev. D* **80**, 016009 (2009)
 - [41] M. Ablikim *et al.* [BES], *Phys. Lett. B* **607**, 243-253 (2005)
 - [42] C. Bourrely, I. Caprini and L. Lellouch, *Phys. Rev. D* **79**, 013008 (2009) [erratum: *Phys. Rev. D* **82**, 099902 (2010)]
 - [43] M. Diehl, T. Gousset, B. Pire and O. Teryaev, *Phys. Rev. Lett.* **81**, 1782-1785 (1998)
 - [44] M. V. Polyakov, *Nucl. Phys. B* **555**, 231 (1999)
 - [45] S. Cheng, *Phys. Rev. D* **99**, no.5, 053005 (2019)
 - [46] L. Y. Dai and M. R. Pennington, *Phys. Rev. D* **90**, no.3, 036004 (2014)
 - [47] L. Y. Dai and U. G. Meißner, *Phys. Lett. B* **783**, 294-300 (2018)
 - [48] S. Faller, T. Feldmann, A. Khodjamirian, T. Mannel and D. van Dyk, *Phys. Rev. D* **89**, no.1, 014015 (2014)
 - [49] E. Kou *et al.* [Belle-II], *PTEP* **2019**, no.12, 123C01 (2019)[erratum: *PTEP* **2020**, no.2, 029201 (2020)]

[50] R. Aaij *et al.* [LHCb], JHEP **12**, 144 (2020)